

Knot Theory and Applications to 3-Manifolds

Emma Schlatter

Submitted to the Department of Mathematics
of Smith College in partial fulfillment
of the requirements for the degree of
Bachelor of Arts with Honors

Elizabeth Denne, Faculty Advisor

May 10, 2010

Acknowledgements

I would like to thank Christophe Gole for his willingness to be the second reader, and for the time and attention he has dedicated to the task; Patricia Sipe for her work as the math department's Director of Honors; my academic advisor Jim Henle, and everyone in the math department, for the academic experiences that prepared me to undertake this project; and especially Elizabeth Denne, my thesis advisor, for her constant guidance and support.

Contents

1	Introduction	1
1.1	Introduction	1
1.2	Preliminaries and Definitions	2
2	Torus Knots	11
2.1	Definitions	11
2.2	Rational Tangles	17
3	Heegaard Splittings	27
3.1	Definition	27
3.2	Examples	30
4	Dehn Twists: Homeomorphisms of 2- and 3-Manifolds	37
4.1	2-Manifolds	37
4.2	3-Manifolds	41
5	Link Surgery	48
5.1	The Dehn-Lickorish Corollary	48
5.2	Link and Ribbon Presentations	51
5.3	Lens spaces, surgery, rational links and covering spaces: two examples	55
6	Conclusion	62

List of Figures

1.1	Three examples of knots, and their catalogue numbers: the unknot 0_1 (left), the trefoil 3_1 (center) and 6_2 (right).	2
1.2	The bachelor's unknotting: a non-ambient isotopy taking the trefoil to the unknot.	3
1.3	Several steps of an isotopy $h : \mathbb{R}^3 \rightarrow \mathbb{R}^3$ which takes one version of the Hopf link to another.	3
1.4	Positive (left) and negative (center) crossings. A link (right) with linking number $+2$.	4
1.5	The three Reidemeister moves.	5
1.6	A band (left) and a Möbius strip (right).	6
1.7	A 2-handlebody (top) and a 4-handlebody (bottom).	8
1.8	Two essential loops in T^2 : the meridian (left) and longitude (center). On the right is an inessential loop. The disk it bounds is shaded.	9
2.1	A coordinate system for T^2 .	12
2.2	The torus knot given by the embedding $k(e^{it}) = (e^{it}, e^{5it})$.	12
2.3	Left: the meridian $k_m(e^{it}) = (1, e^{it})$. Right: the longitude $k_l(e^{it}) = (e^{it}, 1)$.	12
2.4	The preimage of a torus knot k in \mathbb{C} under the covering map p .	13
2.5	The covering q maps the ray δ in $\mathbb{C} \setminus \{0\}$ to a longitude in T^2 , and all three concentric circles γ_1, γ_2 and γ_3 in $\mathbb{C} \setminus \{0\}$ to the same meridian in T^2 .	14
2.6	Liftings of K and K' in $\mathbb{C} \setminus \{0\}$ that bound an annulus.	15
2.7	The covering q maps an isotopy of $\mathbb{C} \setminus \{0\}$ to an isotopy of T^2 . Thus the curves K and K' in T^2 are ambient isotopic.	16
2.8	The Whitehead link and an intersecting sphere (left). The two resulting tangles (right).	17
2.9	Examples of trivial (A) and nontrivial (B) 2-tangles.	18

2.10	The sphere with four points identified (left). Examples of a positive crossing (center) and a negative crossing (right) in a tangle.	19
2.11	The rational tangles t_0 (left) and t_∞ (right).	19
2.12	$H(t_\infty)$ (left), $H^{-3}(t_\infty)$ (center) and $F(t_\infty)$ (right).	20
2.13	The rational tangle $C(5, -2, 3)$	20
2.14	A homeomorphism of (B, α_1, α_2) taking the strands to ∂B	21
2.15	Under the process described in this section, t_0 maps to the meridian.	21
2.16	Three automorphisms of T^2 : the inversion (left), meridional twist (center) and longitudinal twist (right).	22
2.17	Three automorphisms of T^2 : the inversion (left), meridional twist (center) and longitudinal twist (right).	23
3.1	The six small tetrahedra adjacent to one face of a T_i after the first barycentric subdivision.	29
3.2	Left: the shaded region represents the intersection of T_i with K_1 . K_2 is the complement of the shaded region. Right: the ball-and-cylinder model of a portion of K_1	29
3.3	A coordinate system for the solid torus V	30
3.4	A Heegaard splitting $S^3 = (V_1, V_2, h)$. V_1 is visibly a solid torus, and V_2 is a solid torus (shown as a cylinder whose ends meet at the point at infinity). The homeomorphism h maps the longitudes shown on V_1 to meridians shown on V_2	31
3.5	A Heegaard splitting $S^3 = (V_1, V_2, h)$. V_1 is visibly a solid torus, and V_2 is a solid cylinder whose ends meet at the point at infinity. The homeomorphism h maps the longitudes shown on V_1 to meridians shown on V_2	32
3.6	Adding a handle to M_1 in a Heegaard splitting.	32
3.7	The lens S^* . Its boundary consists of the points $(ae^{2\pi i\alpha}, be^{2\pi i\beta}) \in S^*$ with $\alpha = \frac{k}{p}$ or $\alpha = \frac{k}{p+1}$	34
3.8	A Heegaard splitting of the lens into M_1^* and M_2^*	34
3.9	The division of a lens into tetrahedra (left) and the labeled faces of one tetrahedron (right).	35
3.10	An overhead view of the division of a lens into tetrahedra, demonstrating that $L(5, 2) \cong L(5, 3)$	35
4.1	A Dehn twist along a curve γ in a surface S	38

4.2	A homeomorphism of S taking γ_1 to γ_2	39
4.3	Curves α that do not disconnect M^2 , and that intersect γ_1 and γ_2 each once, transversely.	39
4.4	For this γ_1 and γ_2 , either $l \cup \beta_1$ or $l \cup \beta_2$ is the required α	40
4.5	The curves at left are meridians of the solid torus. The ones at right are not. . .	42
4.6	The curves at top are longitudes of the solid torus. The ones at bottom are not. . .	42
4.7	A homeomorphism of a solid torus extended from a homeomorphism of its boundary. . .	43
4.8	Preferred longitudes of two solid tori embedded in S^3	44
4.9	The homeomorphism h of $\mathbb{R}^3 \setminus V$ changes the crossing as shown, and is the identity outside of D	44
4.10	A homeomorphism of $D \setminus V$	45
4.11	Given a knot embedded with a crossing in a solid torus T , choose V as shown and apply Proposition 4.2 to obtain a homeomorphism of $\mathbb{R}^3 \setminus V$ that switches the crossing.	45
4.12	Drilling a hole T in M in preparation for defining a homeomorphism on $M \setminus T$. . .	46
5.1	The spaces of Theorem 5.1, and the maps between them.	49
5.2	$(H = \bigcirc_1 \cup \bigcirc_2; 1, n)$ -surgery.	51
5.3	The effect of the homeomorphism $f : L(p, q) \rightarrow L(p, q+pn)$ on V_2 . In the example, $p = 2$, $q = 1$ and $n = -1$	53
5.4	The effect of a meridional twist of V_2 on the ribbon R_i passing through the center of V_1	54
5.5	A manipulation of link presentations showing that the surgeries given by diagrams (A) and (D) are equivalent.	55
5.6	This surgery gives $L(p, q)$, where $\frac{p}{q}$ is defined below.	56
5.7	The knot K , its Seifert surface M , and the neighborhood $N = N^+ \cup N^-$ in S^3 . . .	57
5.8	A Heegaard splitting of S^3 into balls B_1 and B_2 , which intersect the knot K in pairs of segments A_1 and A_2	58
5.9	An automorphism h_1 of S^2 and its preimage $\tilde{h}_1 \in \text{Aut}(T^2)$ under the covering map $f : T^2 \rightarrow S^2$	59
5.10	A homeomorphism h_2 of ∂B_1 , which yields a meridional twist of ∂T^2	60
5.11	We construct a covering of S^3 over the knot K at left. At right, several steps in the sequence of homeomorphisms of B_1 needed to change A_1 into K	60

Chapter 1

Introduction

1.1 Introduction

This thesis investigates the intersection between knot theory and the theory of 3-manifolds. Knowledge of each subject contributes to an understanding of the other: for instance, 3-manifolds provide the ambient space in which we work with knots, while knot theory allows us to more easily manipulate solid tori in surgery on 3-manifolds.

The classification of torus knots in Chapter 2 is essential for the subsequent material because it allows us to classify homeomorphisms of surfaces (in particular, of the torus) and, later, of the solid torus. Along the way, we reach a classification of rational tangles, which is revisited in a more general form in Chapter 5 with the help of lens spaces and surgery techniques.

Our main goal is to demonstrate a variety of methods for constructing 3-manifolds. In particular, we discuss Heegaard splittings and link and ribbon surgery presentations of 3-manifolds. All of these use knot theory. To understand the homeomorphisms of 3-manifolds that are used in both Heegaard splittings and surgery, it is necessary to understand torus knots. Knowledge of linking number and link equivalence allows us to manipulate link presentations of surgery and to define ribbon presentations.

Lens spaces will be used throughout as illustrations of the methods we describe. The value of lens spaces in this study extends beyond their utility as examples: in Chapter 5, we apply what we have learned about lens spaces to reach small classification results: we show that 3-manifolds obtained by certain types of surgeries are equivalent.

1.2 Preliminaries and Definitions

This chapter introduces some of the basic definitions in knot theory and 3-manifold theory, as well as several motivating examples we will return to in later chapters.

1.2.1 Knots

The definitions here are standard, and can be found in knot theory texts such as [3, 7, 15].

Definition 1. A *knot* is a subset K of \mathbb{R}^3 that is homeomorphic to a circle.

Some examples of knots are shown in Figure 1.2.1. Given a knot K , let k be the homeomorphism from S^1 to \mathbb{R}^3 such that $K = k(S^1)$. Note that since k is a homeomorphism, K has no self-intersections.

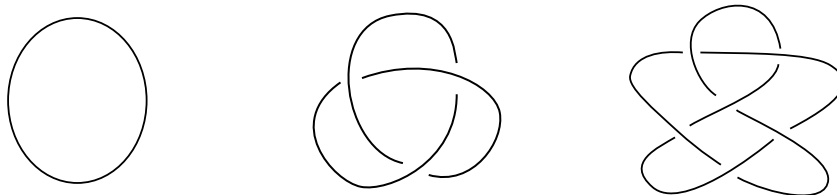


Figure 1.1: Three examples of knots, and their catalogue numbers: the unknot 0_1 (left), the trefoil 3_1 (center) and 6_2 (right).

We will often refer to knot equivalence.

Definition 2. Two knots K and K' are *equivalent* if there is an ambient isotopy between them: that is, an isotopy $h : \mathbb{R}^3 \times [0, 1] \rightarrow \mathbb{R}^3$ with $h(K, 0) = K$ and $h(K, 1) = K'$.

Some equivalence classes of knots have names; all of the ones small enough to be commonly encountered have numbers according to their position in a standard catalogue. All the knots in Figure 1.2.1 belong to different equivalence classes, and their catalogue numbers are given.

Remark 1. Note that the ambient isotopy used in the definition of knot equivalence is a stronger condition than isotopy, because it requires an isotopy of the surrounding space as well as of the knot itself. Simple isotopy is not enough to ensure the type of equivalence we want. The trefoil, for instance, is isotopic to the unknot by a process called bachelor's unknotting, shown in Figure 1.2.1. By requiring an isotopy of the space in which a knot is embedded, we avoid this reduction of nontrivial portions of knots to points.

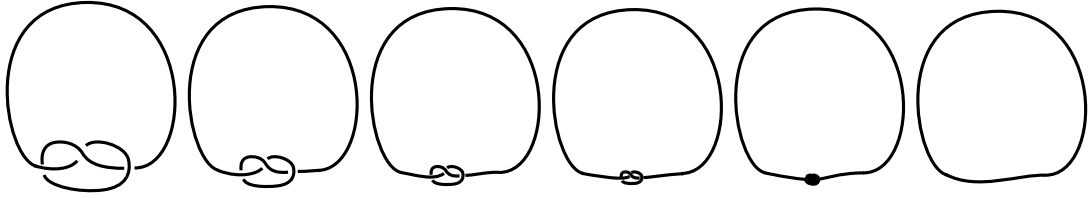


Figure 1.2: The bachelor’s unknotting: a non-ambient isotopy taking the trefoil to the unknot.

In order to exclude certain problematic types of knots, we impose some conditions on the knots to be studied.

Definition 3. A knot is C^1 if, when expressed as a map from the circle to \mathbb{R}^3 , its first derivative exists and is continuous.

Definition 4. A knot is *polygonal* if it is the union of a finite number of line segments intersecting only at their endpoints, with no more than two segments intersecting in a single point.

Definition 5. From this point on, we will consider only knots that are equivalent to a C^1 knot. These are called *tame* knots. (The knots excluded by the condition of equivalence to a C^1 knot are called *wild knots*.)

Remark 2. The condition in Definition 5 is the same as equivalence to a polygonal knot. For the proof that any knot equivalent to a C^1 knot is equivalent to a polygonal knot, see [3]. To see that any knot equivalent to a polygonal knot is equivalent to a C^1 knot, note that a polygonal knot can be transformed into a C^1 knot by an ambient isotopy that rounds the endpoints.

Definition 6. A *link* is a finite union of disjoint knots. The knots that make up a link are called the *components* of the link. (See for instance Figure 1.)

Note that all knots are links. Ambient isotopy can be used to define link equivalence in the same way as for knot equivalence.

Example 1. Figure 1 shows an isotopy of \mathbb{R}^3 demonstrating that L_1 and L_2 are equivalent.

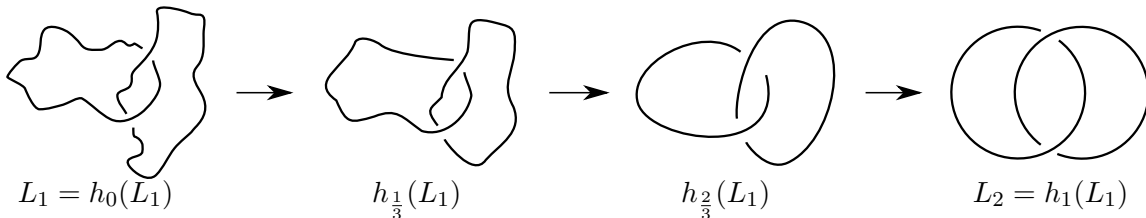


Figure 1.3: Several steps of an isotopy $h : \mathbb{R}^3 \rightarrow \mathbb{R}^3$ which takes one version of the Hopf link to another.

A stronger definition of link equivalence requires specifying which components of the first link

are mapped to which components of the second. But we will use the definition of ambient isotopy, as previously described, unless otherwise specified.

A *link diagram* is a two-dimensional representation of a link, such as the ones we have been using already. We require every crossing point in a link diagram to be transverse (that is, to have a neighborhood homeomorphic to two perpendicular line segments intersecting at their midpoints) and to involve exactly two segments. By distinguishing an upper and lower strand at each crossing, link diagrams contain enough information to identify a link up to equivalence.

Definition 7. A *link invariant* is a map I from the space of link diagrams to some other set S , such that if L_1 and L_2 are equivalent links, then $I(L_1) = I(L_2)$.

Invariants provide a good way to demonstrate the non-equivalence of certain links, since if a given invariant is different for two links, they cannot be equivalent.

Example 2. We define an invariant called linking number. In Figure 1.2.1, the crossing on the left is a *positive crossing*, while the crossing on the right is a *negative crossing*. Given an oriented two-component link diagram $L = K_1 \cup K_2$, choose one component K_1 . The linking number of L is the sum of the signed crossings of K_1 over K_2 . In general, the *linking number* of a link diagram is the sum of the pairwise linking numbers of its components.

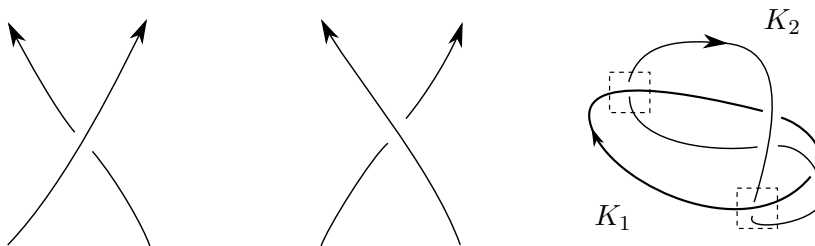


Figure 1.4: Positive (left) and negative (center) crossings. A link (right) with linking number +2.

While invariants are useful for distinguishing nonequivalent links, a set of operations called Reidemeister moves provide a powerful method for proving that two links are equivalent.

Definition 8. The Reidemeister moves are operations performed on link diagrams. They are shown in Figure 8.

Theorem 1.1. *Two link diagrams are equivalent if one can be obtained from the other by a finite series of Reidemeister moves and isotopies of the plane.* □

(See for instance [3, 17, 19] for proof.) Thus, proving that a property is a link invariant can be reduced to proving that it is unchanged by Reidemeister moves. As an example, we show that

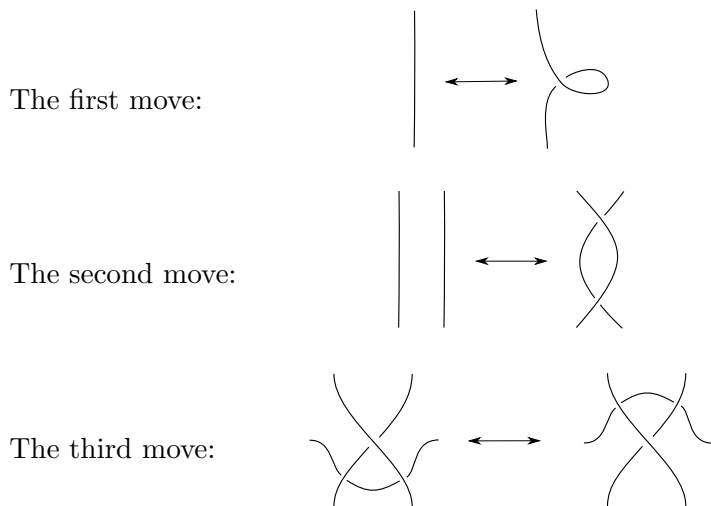


Figure 1.5: The three Reidemeister moves.

linking number is an invariant.

Proposition 1.1. *If two link diagrams are equivalent, they have the same linking number.*

Proof. It suffices to show that the three Reidemeister moves do not change linking number.

1. Since the first Reidemeister move involves only one component of a link, it does not change the linking number.
2. Suppose the two strands in the diagram of the second move belong to separate components of the link (if they belong to the same component, then the linking number will not change). The two crossings on the right in the diagram of the second move in Figure 8 are of opposite signs, so both the left and right diagrams have linking number 0.
3. The third move does not add or remove any crossings, so the linking number is not changed.

□

1.2.2 Manifolds

There are several definitions and concepts we will need from topology. These are also standard, and can be found in texts such as [1, 9, 16].

Definition 9. An n -manifold M^n (or simply M) is a Hausdorff space such that each point has an open neighborhood which is homeomorphic to \mathbb{R}^n . An n -manifold with boundary is

locally homeomorphic to $\mathbb{R}_+^n = \{(x_1, x_2, \dots, x_n) \in \mathbb{R}^n \mid x_n \geq 0\}$. The *boundary* (∂M^n or ∂M) of such a manifold consists of those points that map to the set $\{(x_1, x_2, \dots, x_n) \mid x_n = 0\}$ in a homeomorphism from M^n to \mathbb{R}_+^n .

Example 3. $\mathbb{R}_+ = \{r \in \mathbb{R} \mid r \geq 0\}$, the positive real line, is a 1-manifold with boundary $\{0\}$.

Example 4. $S^1 = \{(x, y) \in \mathbb{R}^2 \mid x^2 + y^2 = 1\}$, the unit circle, is a 1-manifold with empty boundary.

Definition 10. A *surface* is a compact 2-manifold.

Example 5. $S^2 = \{(x, y, z) \in \mathbb{R}^3 \mid x^2 + y^2 + z^2 = 1\}$ is a surface with empty boundary.

Example 6. The *torus* is the surface $T^2 = S^1 \times S^1$. It also has empty boundary.

Next, we discuss two important properties of manifolds: orientability and genus. The definition of orientability is given for general n -manifolds, while we will define genus only for surfaces and orientable 3-manifolds. Taken together, these two properties allow for a complete classification of surfaces.

Definition 11. An *orientation* of a point in an n -manifold is a choice of positive direction in each of the n dimensions. A manifold M is *orientable* if it is possible to assign an orientation to every point in M in such a way that every closed loop in M has a consistent orientation.

Example 7. Pictured in Figure 7 are two 2-manifolds with boundary. The band (left) is orientable, while the Möbius strip (right) is not.

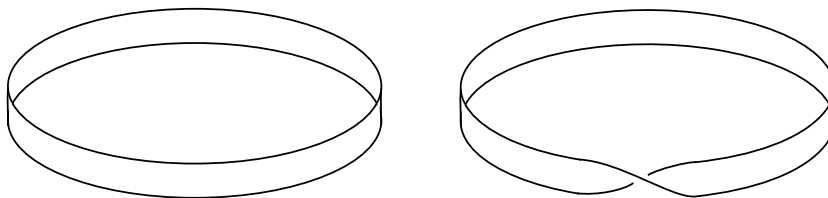


Figure 1.6: A band (left) and a Möbius strip (right).

Definition 12. Given a surface M^2 , a surface T homeomorphic to M^2 is a *triangulation* of M^2 if T consists of triangles whose pairwise intersection is an entire edge, a vertex, or \emptyset .

The following propositions, stated here without proof (see [1, 4, 9, 16]), are necessary for the definition of genus to follow.

Proposition 1.2. *Every surface has a triangulation.* □

Proposition 1.3. *Let V be the number of vertices, E the number of edges and F the number of faces (triangles) in a triangulation of M^2 . Then the quantity $\chi(M^2) = V - E + F$ (called the Euler characteristic of M^2) is a topological invariant.* □

Definition 13. The quantity $g(M^2) = 1 - \frac{1}{2}(\chi(M^2) + |\partial(M^2)|)$ (where $|\partial(M^2)|$ is the number of boundary components of M^2) is the *genus* of the surface M^2 . The *genus* of an orientable 3-manifold is the genus of its boundary.

Remark 3. Intuitively, the genus of a surface can be thought of as the number of handles that must be attached to a sphere to obtain it. For instance, the surface in Figure 9A has genus 2, while the surface in Figure 9B has genus 4.

The following theorem provides a complete classification of surfaces using the invariants orientability and genus.

Theorem 1.2 (Classification Theorem for Surfaces). *Every compact, path-connected surface M^2 is homeomorphic to S^3 or a connected sum of tori (if M^2 is orientable) or a connected sum of projective planes (if M^2 is nonorientable).* \square

Now we turn our attention to 3-manifolds. The most basic example of a 3-manifold is \mathbb{R}^3 . Another example which will arise frequently is S^3 .

Example 8. The 3-sphere (written S^3) has many equivalent definitions [3]. We give three of them.

1. Generalizing from the definitions of S^1 and S^2 as subsets of \mathbb{R}^2 and \mathbb{R}^3 , respectively, we can define S^3 as the subset of points in \mathbb{R}^4 with length 1:

$$S^3 = \{(x_1, x_2, x_3, x_4) \in \mathbb{R}^4 \mid x_1^2 + x_2^2 + x_3^2 + x_4^2 = 1\}.$$

We will often find it more convenient, however, to consider S^3 as a subset of \mathbb{C}^2 :

$$S^3 = \{(ae^{i\alpha}, be^{i\beta}) \mid a^2 + b^2 = 1\}.$$

2. An important difference between \mathbb{R}^n and S^n is that S^n is compact, while \mathbb{R}^n is not. Define $S^n = \mathbb{R}^n \cup \{\infty\}$, where $U \subset S^n$ is open if and only if either U is open in \mathbb{R}^3 or the complement of $U \setminus \{\infty\}$ in \mathbb{R}^3 is closed and bounded. Since the addition of the point at infinity transforms \mathbb{R}^n into a compact space, this definition of S^n is known as the *one-point compactification* of \mathbb{R}^n .
3. Gluing two 3-disks B_1 and B_2 together by a homeomorphism $h : \partial B_1 \rightarrow \partial B_2$ also yields S^3 . This is the first example of a Heegaard splitting. We will investigate Heegaard splittings further in Chapter 3.

Example 9. The solid torus $V = D^2 \times S^1$ is our first example of a 3-manifold with boundary. Its boundary surface is the torus of Example 6. Solid tori will be important in later chapters as

a way to represent knots. In Section 3.2, we will see a way to write the solid torus as a subset of \mathbb{C}^2 .

The g -*handlebody*, a generalization of the solid torus, is a 3-manifold M such that ∂M is an orientable surface of genus g .

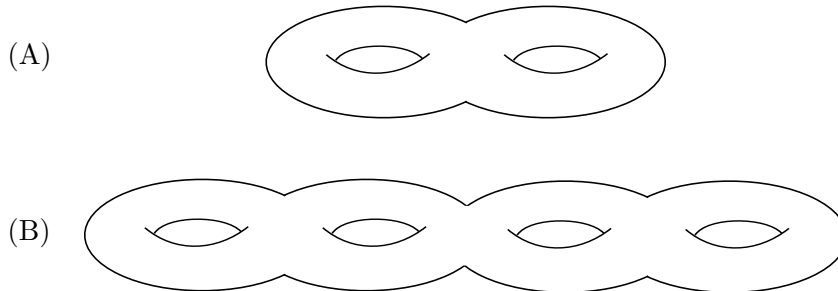


Figure 1.7: A 2-handlebody (top) and a 4-handlebody (bottom).

3-manifolds are important in knot theory because they often provide the ambient space in which knots are studied. So far, we have considered knots as subsets of \mathbb{R}^3 . But it is often more convenient to consider a knot within a different 3-manifold, particularly S^3 . To make this precise, we need the concept of an embedding.

Definition 14. Let X and Y be manifolds. Then X is *embedded* in Y if there is a homeomorphism $h : X \rightarrow h(X) \subset Y$ such that the topology on $h(X)$ inherited from X matches the subspace topology of $h(X)$ in Y . Such a homeomorphism is called an *embedding*.

A knot is an example of an embedding of S^1 in \mathbb{R}^3 . We can now also define a knot as an embedding of a circle in S^3 , or any other 3-manifold.

Embeddings also occur in 2-manifolds. A *loop* is a circle embedded in a surface. Torus knots are an example of this:

Example 10. A *torus knot* is an embedding of S^1 in T^2 . A more detailed definition will follow in Section 2.1. An understanding of torus knots has useful applications. We will see one of these —the classification of rational tangles — in Section 2.2. Torus knots will also be important in our discussion of automorphisms of the torus and, later, surgery of 3-manifolds.

Definition 15. A curve γ embedded in a connected surface M^2 is *separating* if $M^2 \setminus \gamma$ is disconnected. Otherwise, γ is *nonseparating*.

Definition 16. An *essential* loop in a surface M^2 is a loop that does not bound a disk in M^2 .

Example 11. The torus has two types of essential loops, called *meridians* and *longitudes*, shown in Figure 11. These will be very important in the material to follow, and they will be defined

more precisely in Section 2.1. Figure 11 also shows an inessential loop in T^2 .

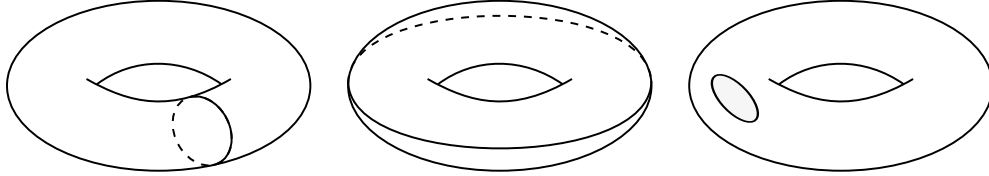


Figure 1.8: Two essential loops in T^2 : the meridian (left) and longitude (center). On the right is an inessential loop. The disk it bounds is shaded.

1.2.3 An introduction to lens spaces

Lens spaces are a class of 3-manifolds that will frequently recur as examples in the chapters to come. There are many equivalent ways to define lens spaces, and we will see several of them as lens spaces appear in different contexts. We introduce them in this subsection by defining them as spaces covered by S^3 . To do this requires some covering space theory, which can be found in [6, 16].

Definition 17. Let X and Y be topological spaces, and $p : X \rightarrow Y$ a map between them. Then p is a *covering map* if:

- p is continuous, and
- For all $x \in X$, there exists an open neighborhood U of x such that $p^{-1}(U) = \bigcup N_i$ for disjoint open sets N_i , with $p|_{N_i}$ a homeomorphism for all i .

Definition 18. Given a group G and a space Y , an *action* of G on Y is a map from $G \times Y$ to Y such that:

- $(g_1 g_2) \cdot y = g_1 \cdot (g_2 \cdot y)$ for all $g_1, g_2 \in G$ and $y \in Y$.
- For the identity element $e \in G$, $e \cdot y = y$ for all $y \in Y$.
- For any $g \in G$, the restriction of the action to a map $\{g\} \times Y \rightarrow Y$ is a homeomorphism of Y .

Let $p : Y \rightarrow Y/G$ be the map such that $p(y) = \{g \cdot y \mid g \in G\}$, and give Y/G the quotient topology: $U \subset Y/G$ is open if and only if $p^{-1}(U) \subset Y$ is open.

Definition 19. A group action is *even* if for all $y \in Y$, there exists a neighborhood V of y such that $(g_1 \cdot V) \cap (g_2 \cdot V) = \emptyset$ for all $g_1 \neq g_2 \in G$.

Proposition 1.4. *If a group action $G \times Y \rightarrow Y$ is even, then the map $p : Y \rightarrow Y/G$ is a covering map.* □

Example 12. Let G be the group of n th roots of unity, for n a prime number. Define Y to be $S^3 \subset \mathbb{C}^2$, as in Definition 1 of Example 8: $Y = \{(z_1, z_2) \in \mathbb{C}^2 \mid |z_1|^2 + |z_2|^2 = 1\}$. Then define a group action of G on Y by $\zeta \cdot (z_1, z_2) = (\zeta z_1, \zeta z_2)$ for $\zeta \in G$ and $(z_1, z_2) \in Y$.

Consider the effect of this action on a point $y \in Y$. Suppose ζ is the n th root of unity $e^{2\pi ik/n}$ and $y = (r_1 e^{i\theta}, r_2 e^{i\phi})$. Then $\zeta \cdot y = (r_1 e^{i(\theta+2\pi ik/n)}, r_2 e^{i(\phi+2\pi ik/n)})$: that is, ζ rotates each coordinate of y by $2\pi ik/n$. This is an even action. So, by Proposition 1.4, p is a covering map.

Definition 20. The space Y/G is called a *lens space*.

Chapter 2

Torus Knots

Torus knots are knots embedded in the surface of the torus. In this chapter, we will classify the torus knots by their representative elements in $H_1(T^2)$, the simplicial first homology with integer coefficients. By associating torus knots with a class of objects known as rational tangles, we will then reach a classification of rational tangles. The classification of torus knots is also necessary background for the surgery techniques that will be developed in Chapters 4 and 5.

2.1 Definitions

We begin this section with a parametrization of S^1 in T^2 that yields a family of torus knots. The proof of part 1 of Theorem 2.1 shows which constants in the parametrization actually give torus knots, and which elements of $H_1(T^2)$ each parametrization represents. Theorem 2.1 also states that homotopic torus knots represent the same element of $H_1(T^2)$. Thus we'll find that each homotopy class of torus knots can be identified by an element of $H_1(T^2)$, or by a choice of constants in the parametrization.

In order to define torus knots parametrically, first assign coordinates to the torus. Let θ be the angle measured from the center, and ϕ be the angle measured from the core. Then any point on the torus can be uniquely expressed as $(e^{i\theta}, e^{i\phi})$, for $\theta, \phi \in [0, 2\pi]$.

Now we can represent torus knots as embeddings of S^1 in T^2 . Here, we'll use the unit circle in \mathbb{C} , that is, $S^1 = \{e^{it} : t \in [0, 2\pi]\}$. So a knot is given by a homeomorphism $k : S^1 \rightarrow T^2$. For example, the function $k(e^{it}) = (e^{it}, e^{5it})$ produces the knot in Figure 2.1.

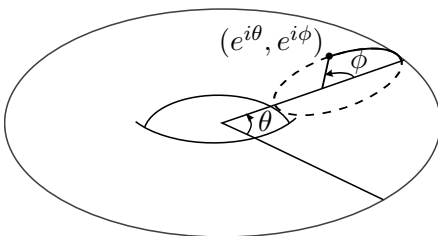


Figure 2.1: A coordinate system for T^2 .

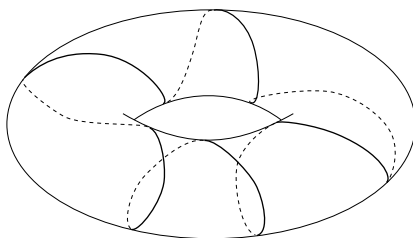


Figure 2.2: The torus knot given by the embedding $k(e^{it}) = (e^{it}, e^{5it})$.

Definition 21. The *meridian* and *longitude* of the torus are torus knots with representative functions $k_m(e^{it}) = (1, e^{it})$ and $k_l(e^{it}) = (e^{it}, 1)$, respectively, as shown in Figure 2.1.

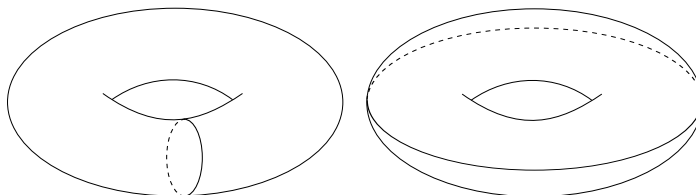


Figure 2.3: Left: the meridian $k_m(e^{it}) = (1, e^{it})$. Right: the longitude $k_l(e^{it}) = (e^{it}, 1)$.

Since torus knots are loops in T^2 , they all represent elements of the simplicial homology $H_1(T^2)$. We make frequent use of the fact that $H_1(T^2) = \mathbb{Z} \oplus \mathbb{Z}$ and that it is generated by elements representing the meridian and longitude of T^2 . Letting $[k_m] = \langle 0, 1 \rangle$ and $[k_l] = \langle 1, 0 \rangle$, for every torus knot k we have $[k] = \langle a, b \rangle$ for some $a, b \in \mathbb{Z}$.

Which elements $\langle a, b \rangle$ of $H_1(T^2)$ can be represented by torus knots, and when do two torus knots k_1 and k_2 represent the same element of $H_1(T^2)$?

Theorem 2.1. 1. A homeomorphism $k : S^1 \rightarrow T^2$ such that $[k] \in \langle a, b \rangle$ exists if and only if $\gcd(a, b) = 1$ or $a = b = 0$.

2. Any homotopy between knots in the torus can be extended to an isotopy on all of T^2 : that is, torus knots that are homotopic in T^2 are also ambient isotopic.

Proof. This proof follows arguments given in [17] and [20].

1. We use the covering map $\mathbb{C} \xrightarrow{p} T^2$, with $p(x+iy) = (e^{ix}, e^{iy})$. This gives the complex plane with the identifications $x_1 + iy_1 = x_2 + iy_2$ whenever $x_1 \equiv x_2$ and $y_1 \equiv y_2 \pmod{2\pi}$.

Suppose $\gcd(a, b) = 1$ or $a = b = 0$. In the latter case, note that $\langle 0, 0 \rangle$ is represented by any inessential loop in the torus (such as the one in Figure 11), which can be expressed as $k_0(S^1)$ for some homeomorphism $k_0 : S^1 \rightarrow T^2$. Next, address the case in which $\gcd(a, b) = 1$. Let $k(e^{it}) = (e^{ait}, e^{ibt})$, $t \in [0, 2\pi]$. Consider the lifting $\tilde{k}(e^{it}) = (at + ibt)$ of k under p . In \mathbb{C} , \tilde{k} traces the line segment $\{at + ibt | t \in [0, 2\pi]\}$ from $(0, 0)$ to (a, b) . So k is a homeomorphism when $\gcd(a, b) = 1$ (and only then: if $\gcd(a, b) = n > 1$, then $p \circ \tilde{k}(2\pi/n) = p(2\pi a/n + i(2\pi b/n)) = p(2\pi a, 2\pi b) = p \circ \tilde{k}(2\pi)$ as shown in Figure 1, contradicting the injectivity of k).

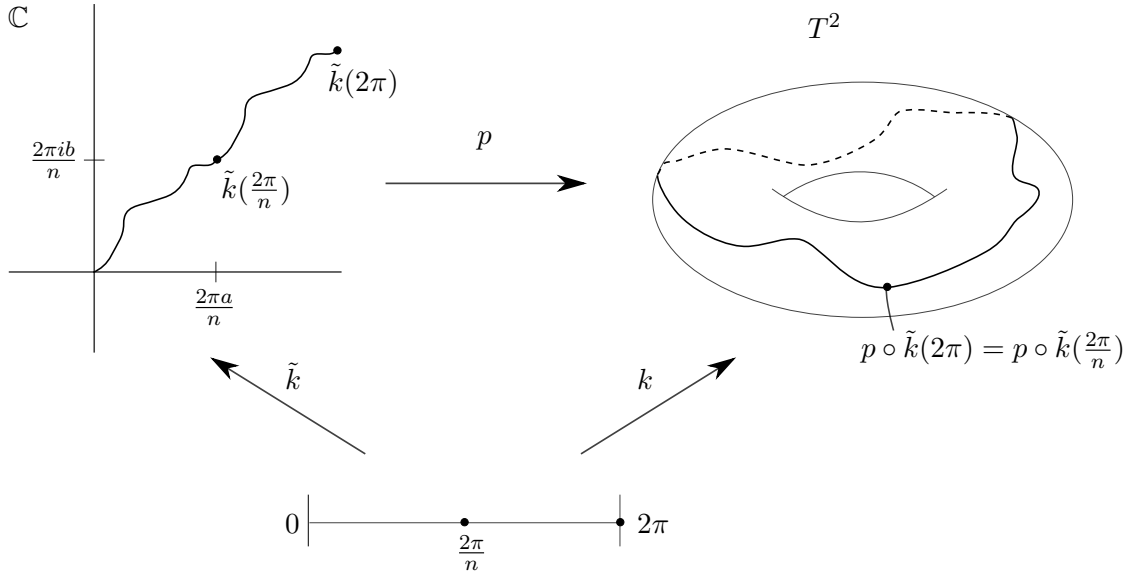


Figure 2.4: The preimage of a torus knot k in \mathbb{C} under the covering map p .

A proof of the following lemma can be found in [20].

Lemma 2.1 (The Chord Theorem). *Let γ be a path in \mathbb{C} , and T be a segment of length $|T|$ with endpoints on γ . For all $n \in \mathbb{Z}_{>0}$, there exists a segment parallel to T of length $\frac{|T|}{n}$ with endpoints on γ . \square*

Now suppose $\gcd(a, b) = n > 1$. Show that there cannot be a homeomorphism $k : S^1 \rightarrow T^2$ such that $[k] = \langle a, b \rangle$. For, suppose such a k exists. Consider a lifting \tilde{k} of k . There is a

chord α with its endpoints $(0, 0)$ and $(2\pi a, 2\pi b)$ on \tilde{k} . So, by the Chord Theorem, there must exist a chord parallel to α with length $(1/n)|\alpha|$ and endpoints on \tilde{k} . That is, there exist s, t in $[0, 2\pi]$ such that $\tilde{k}(s) - \tilde{k}(t)$ is such a chord, which can be written $2\pi/n(a+bi) = 2\pi((a/n) + i(b/n))$. Since a/n and b/n are integers, $k(s) = p \circ \tilde{k}(s) = p \circ \tilde{k}(t) = h(t)$, so k is not a homeomorphism.

2. To show that knots homotopic in T^2 are ambient isotopic in T^2 , we prove a series of lemmas. They use the covering $q(re^{i\theta}) = (e^{ir}, e^{i\theta})$ from $\mathbb{C} \setminus \{0\}$ to T^2 shown in Figure 2:

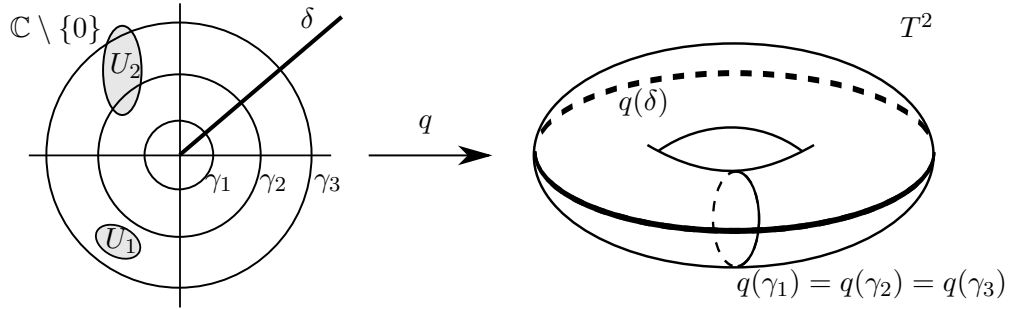


Figure 2.5: The covering q maps the ray δ in $\mathbb{C} \setminus \{0\}$ to a longitude in T^2 , and all three concentric circles γ_1 , γ_2 and γ_3 in $\mathbb{C} \setminus \{0\}$ to the same meridian in T^2 .

Also necessary to the following lemmas is the notion of a *fundamental region* of a covering:

Definition 22. Let $p : X \rightarrow Y$ be a covering. Then $U \subset X$ lies in a *fundamental region* if p restricted to some neighborhood of U is a homeomorphism.

For example, in Figure 2, U_1 lies in a fundamental region but U_2 does not.

Remark 4. Let $p : X \rightarrow Y$ be a covering map. If $U \subset X$ lies in a fundamental region and two paths are ambient isotopic in U , then their images are ambient isotopic in Y (by the isotopy of $p(U)$ given by composing the isotopy of U with the covering map restricted to U).

Lemma 2.2. If K and K' are disjoint torus knots represented by $\langle 1, 0 \rangle \in H_1(T^2)$, then they are ambient isotopic.

Proof. There is a choice of liftings \tilde{K} and \tilde{K}' of K and K' by q that bound an annulus in $\mathbb{C} \setminus \{0\}$ such that the annulus contains no other liftings of K or K' in its interior, as shown in Figure 2. Then \tilde{K} and \tilde{K}' must be ambient isotopic, since they bound an annulus. The condition of no other liftings in the interior ensures that the annulus must lie in a fundamental region. Thus $q(\tilde{K}) = K$ and $q(\tilde{K}') = K'$ are ambient isotopic. \square

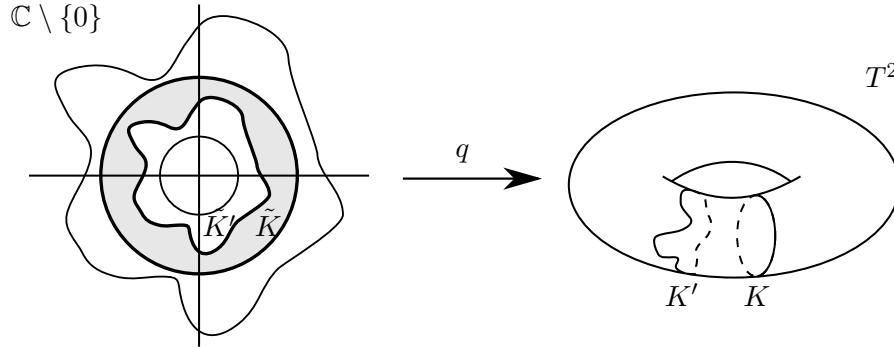


Figure 2.6: Liftings of K and K' in $\mathbb{C} \setminus \{0\}$ that bound an annulus.

Lemma 2.3. *Suppose K is represented by $\langle \pm 1, 0 \rangle \in H_1(T^2)$ and has a finite number of intersections with the meridian $m(t) = (1, e^{it})$, all of which are transverse. Then K and m are ambient isotopic.*

Proof. Consider a lifting \tilde{K} of K by q and the preimage of the meridian $q^{-1}(m)$, as shown in Figure 2(A). There is exactly one crossing of \tilde{K} and $q^{-1}(m)$ for each crossing of K and m . We reduce this to the case of Lemma 2.1 by the following procedure:

Choose a point $z \in \tilde{K}$ such that $|z|$ is maximal. By ambient isotopy, we can transform \tilde{K} to remove the crossings $\tilde{K} \cap q^{-1}(m)$ near z and obtain a curve like the one shown in Figure 2(B). We show that such an isotopy of $\mathbb{C} \setminus \{0\}$ maps to an isotopy of T^2 .

Let J be the component of $\tilde{K} \setminus q^{-1}(m)$ that contains z . Then J , together with an arc of one of the components of $q^{-1}(m)$, bounds a disk D in $\mathbb{C} \setminus \{0\}$. Note that $q|_{\partial D}$ is a homeomorphism, since q is a homeomorphism when restricted to \tilde{K} or to any single component of $q^{-1}(m)$ (a lifting of m). So the homeomorphism can be extended to the interior of D : that is, D lies in a fundamental region. Thus the ambient isotopy of \tilde{K} maps to an ambient isotopy of K . The results of both these isotopies are shown in Figure 2(B).

Each such ambient isotopy decreases the size of $\tilde{K} \cap q^{-1}(m)$ (and, correspondingly, of $K \cap m$) by at least two. So a finite number of ambient isotopies reduces this case to the one in Lemma 2.1. \square

Given any torus knot K of type $\langle \pm 1, 0 \rangle \in H_1(T^2)$, small perturbations reduce the intersection of K and m to a finite set of transverse crossings. Thus we have proven that all knots of type $\langle \pm 1, 0 \rangle$ are ambient isotopic as sets to the meridian, so (by composition of isotopies) any two knots of type $\langle \pm 1, 0 \rangle$ are ambient isotopic as sets.

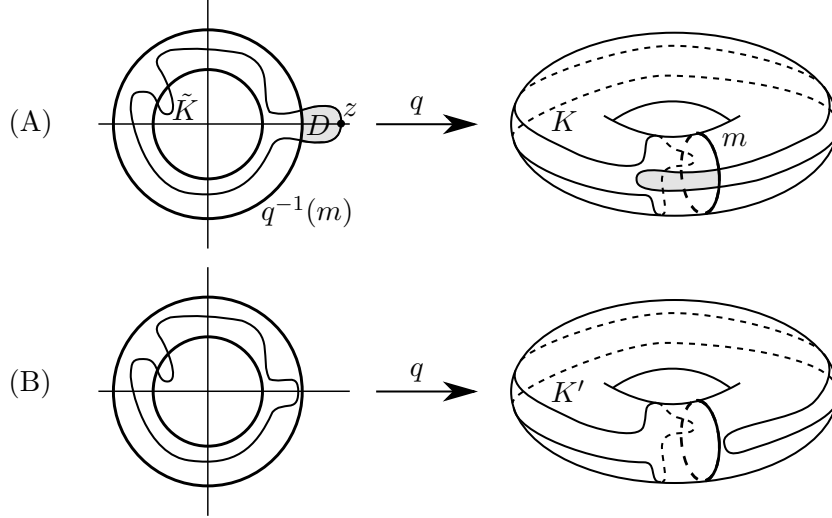


Figure 2.7: The covering q maps an isotopy of $\mathbb{C} \setminus \{0\}$ to an isotopy of T^2 . Thus the curves K and K' in T^2 are ambient isotopic.

In general, given two homotopic knots K and K' of class $\langle p, q \rangle$ (we can assume by part 1 that p and q are relatively prime), we construct a homeomorphism $h : T^2 \rightarrow T^2$ such that the induced group homomorphism $h_* : H_1(T^2) \rightarrow H_1(T^2)$ maps $\langle a, b \rangle$ to $\langle \pm 1, 0 \rangle$. Then applying the previous lemma to $h(K)$ and $h(K')$, use h^{-1} to obtain an ambient isotopy of K and K' .

Define h as follows. Suppose $|p| \geq |q|$. Then by the Euclidean division algorithm, letting $p = x_{-1}$ and $q = x_0$:

- $x_{-1} = n_1 x_0 + x_1$, where $x_1 < x_0$.
- $x_0 = n_2 x_1 + x_2$, where $x_2 < x_1$.
- \vdots
- $x_{k-3} = n_{k-1} x_{k-2} + x_{k-1}$, where $x_{k-1} < x_{k-2}$.
- $x_{k-2} = n_k x_{k-1}$, where $x_{k-1} = \gcd(p, q)$.

For each step i of the division algorithm, perform a homeomorphism h_i defined as follows. If i is even, let h_i be the homeomorphism that takes knots of class $\langle x_{i-2}, x_{i-1} \rangle$ to knots of class $\langle x_{i-2} - n_i x_{i-1}, x_{i-1} \rangle = \langle x_i, x_{i-1} \rangle$. (In the next section, we will see that this homeomorphism is n_i reverse longitudinal twists.) If i is odd, h_i is the homeomorphism that takes knots of class $\langle x_{i-1}, x_{i-2} \rangle$ to knots of class $\langle x_{i-1}, x_{i-2} - n_i x_{i-1} \rangle = \langle x_{i-1}, x_i \rangle$.

(This homeomorphism will be a succession of meridional twists.)

Then $h_k \circ \cdots \circ h_1$ takes a knot of class $\langle p, q \rangle$ to a knot of class $\langle 0, x_{k-1} \rangle$ or $\langle x_{k-1}, 0 \rangle$ (depending on the parity of k). By assumption, $x_{k-1} = \gcd(p, q) = 1$. Thus $h = h_k \circ \cdots \circ h_1$ takes K and K' either to meridians or to longitudes. In the former case, the claim is proven. In the latter, composing h with an inversion (a homeomorphism which will be defined in the next section) yields a homeomorphism mapping K and K' to meridians.

If $|p| < |q|$, let $p = x_0$ and $q = x_{-1}$, reverse the roles of the even and odd i 's, and repeat the process above.

□

2.2 Rational Tangles

Torus knots can be used to classify a set of objects known as rational tangles. There is also a more general classification of rational links [11], which has connections with the surgery techniques we'll develop in Chapters 4 and 5. The following material is originally due to Conway [2] and can also be found in [3, 8, 12].

Definition 23. Given a link L and a sphere S that intersects L transversely in $2n$ points, where S bounds two balls B_1 and B_2 in \mathbb{R}^3 , $(B_i, L \cap B_i)$ is an n -tangle for $i = 1, 2$. For a chosen S , the two tangles $(B_1, L \cap B_1)$ and $(B_2, L \cap B_2)$ are called a *tangle decomposition* of L .

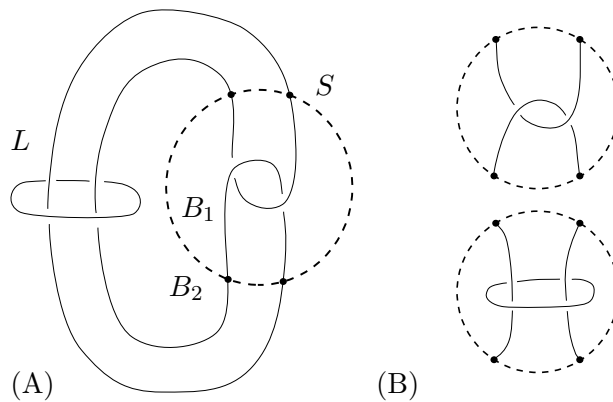


Figure 2.8: The Whitehead link and an intersecting sphere (left). The two resulting tangles (right).

Example 13. The *trivial n -tangle* is homeomorphic to a cylinder containing n straight strands, each of which intersects both the top and bottom faces.

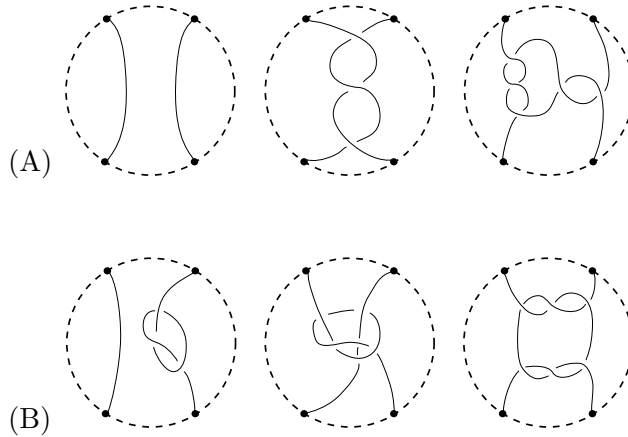


Figure 2.9: Examples of trivial **(A)** and nontrivial **(B)** 2-tangles.

Note: It is convenient to think of a homeomorphism of tangles as sliding the endpoints of the strands around on the sphere. Although any homeomorphism of a tangle can be visualized this way, it is important to note that a homeomorphism of a tangle is a homeomorphism of all of B .

Definition 24. A *rational tangle* is a trivial 2-tangle.

The notion of rational tangle is used to define a rational link: one which decomposes into two rational tangles. Rational links have been extensively studied [3, 12, 23] We will see them again in Section 5.3.

We will focus on rational tangles. Since they are 2-tangles, the strands intersect the sphere in 4 points. It is useful to be able to distinguish these points, so we label them with cardinal directions: NW, NE, SE, SW. (See Figure 2.10.)

Definition 25. Two tangles will be considered *equivalent* if one can be obtained from the other by an isotopy of the strands that fixes their boundaries (the four points on the sphere).

Remark: this definition of equivalence is stronger than homeomorphism. All rational tangles are homeomorphic (since they are trivial, and thus by definition homeomorphic to the cylinder with straight lines) but, as we will see, not all are equivalent.

Definition 26. We'll need a way to describe the direction of twists in a tangle. The crossing on the left of Figure 2.10 is called a *positive crossing*, while the crossing on the right is a *negative crossing*.

Remark 5. This definition is analogous to the definition of positive and negative crossings in oriented links, with the property of orientation replaced with labeled fixed points.

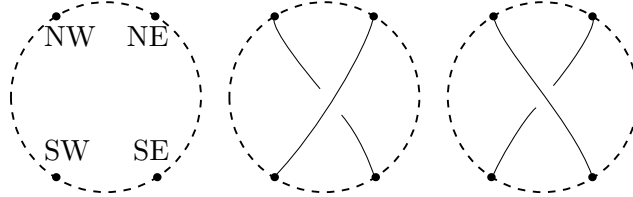


Figure 2.10: The sphere with four points identified (left). Examples of a positive crossing (center) and a negative crossing (right) in a tangle.

Example 14. There are two rational tangles that contain no twists. They are called t_0 and t_∞ , and they are pictured below. Note that t_0 and t_∞ are not equivalent: there is no boundary-fixing isotopy of the strands that maps one to the other.

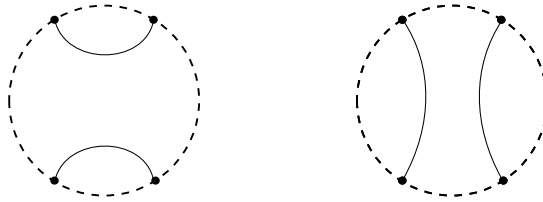


Figure 2.11: The rational tangles t_0 (left) and t_∞ (right).

Next, define two operations on rational tangles.

H : give the NE and SE ends a half-twist, to create a positive crossing.

F : reflect the tangle through the plane containing the points NW and SE, and orthogonal to the plane of the diagram.

We'll write these operations as functions; for instance, on a rational tangle t , performing the operation H is written $H(t)$, performing F and then H is $H(F(t))$, and performing H , n times in succession, is $H^n(t)$.

This allows the creation of infinitely many non-equivalent tangles: t_0 , $H(t_0)$, $H^2(t_0)$ and in general $H^n(t_0)$ ($n \in \mathbb{N}$) are all non-equivalent.

Note that H and F have well-defined inverses. H^{-1} gives a negative half-twist to the NE and SE ends, while $F^{-1} = F$. So $H^{-n}(t)$ will be n repetitions of H^{-1} , for $n \in \mathbb{N}$.

Conway's algorithm is a procedure for creating more complicated tangles from t_0 and t_∞ . Given

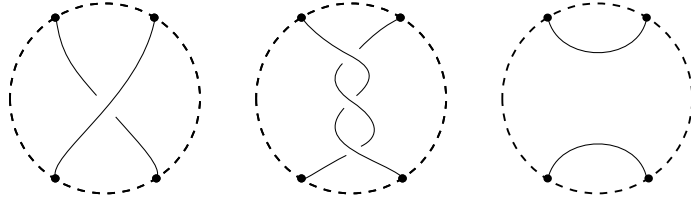


Figure 2.12: $H(t_\infty)$ (left), $H^{-3}(t_\infty)$ (center) and $F(t_\infty)$ (right).

a sequence of integers a_1, a_2, \dots, a_n , Conway's algorithm does the following:

- Begin with $t = t_\infty$.
- For each i from n to 1, let $t := H^{a_i}(F(t))$.

The resulting tangle is written as $C(a_1, a_2, \dots, a_n)$. For example, the tangle $C(5, -2, 3)$ is shown in Figure 2.13.

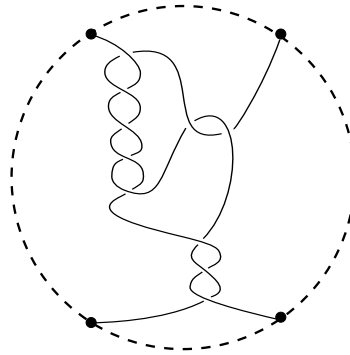


Figure 2.13: The rational tangle $C(5, -2, 3)$.

Different sequences of integers can produce equivalent tangles. When are two tangles generated by the algorithm equivalent? We next develop a classification of rational tangles by associating them with elements of $GL(2, \mathbb{Z})$.

Using the four marked points, create a branched covering of the tangle's sphere by a torus as follows: let $\rho : T \rightarrow T$ be a rotation by π , and $x \sim y$ iff $\rho(x) = y$ (note that this is an equivalence relation). Now define T / \sim to be the *4-point sphere*. Then $p : T \rightarrow T / \sim$ where $p(x) = \{x, \rho(x)\}$ is a branched covering. (We will see branched coverings again in more detail in Section 5.3.)

Let the two strands of $B \cap L$ be written α_1 and α_2 . Their endpoints are at the branch points of T / \sim . Construct an isotopy of the tangle which moves α_1 and α_2 to the boundary of the 4-

point sphere. By definition of a rational tangle, there is a homeomorphism f taking $(B, \alpha_1 \cup \alpha_2)$ to the cylinder with two straight, untwisted strands. These two strands can easily be moved to the boundary of the cylinder. Let R_i denote the area each α_i passes through in the shortest such move to the boundary. R_i is a rectangle in B , and R_1 and R_2 are clearly disjoint. Since f is a homeomorphism of B , $f^{-1}(R_1)$ and $f^{-1}(R_2)$ are disjoint as well. Each $f^{-1}(R_i)$ has α_i as one of its edges, and a curve α'_i along the boundary of B as its opposite edge. So we have the desired isotopy moving α_i through $f^{-1}(R_i)$ to α'_i (see Figure 2.2). The result is a tangle $(B, \alpha'_1 \cup \alpha'_2)$, equivalent to the original, with strands on the boundary of B .

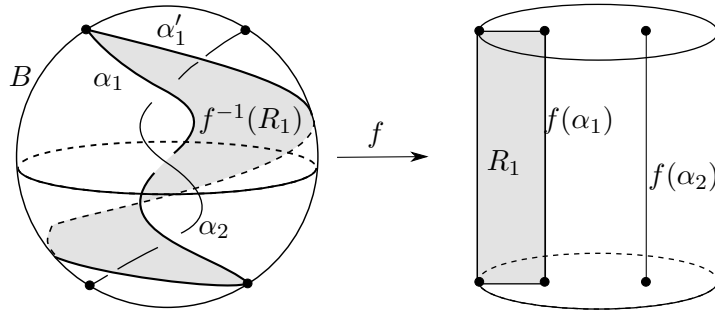


Figure 2.14: A homeomorphism of (B, α_1, α_2) taking the strands to ∂B .

Now, examine the pre-images of α_1 and α_2 under the covering $p : T \rightarrow T/\sim$. Since the endpoints of the strands are branch points of the covering, they are fixed by p , so the pre-image of each strand is a closed curve in T . So $p^{-1}(\alpha_1) = p^{-1}(\alpha_2) = T(a, b)$ for some $a, b \in \mathbb{Z}$. Thus we have created a map from the space of rational tangles to the space of torus knots. Let $t_{a/b}$ be the tangle that maps to $T(a, b)$.

The logic of this notation in general will soon become clear. In particular, Figure 2.2 demonstrates that t_0 will map to $T(0, 1)$ (the meridian of the torus); similarly, t_∞ (or $t_{1/0}$) maps to $T(1, 0)$ (the longitude).

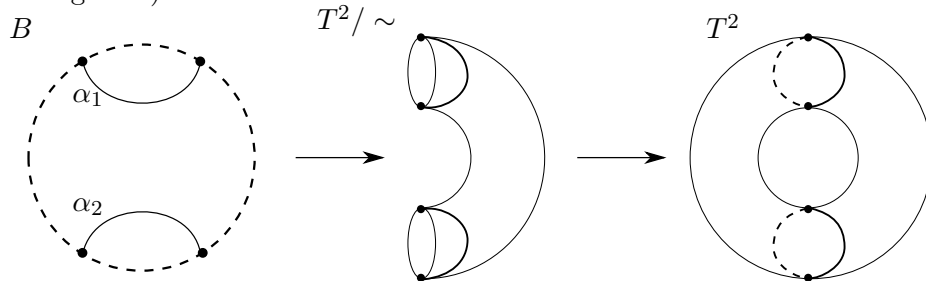


Figure 2.15: Under the process described in this section, t_0 maps to the meridian.

Now we'll associate tangle operations with automorphisms of the torus, and then define a map $\Phi : \text{Aut}(T) \rightarrow \text{GL}(2, \mathbb{Z})$. Consider $\text{Aut}(T) = \{h : T \rightarrow T \mid h \text{ is a homeomorphism}\}$, the group of automorphisms of the torus. Its elements include:

- the inversion $(e^{i\theta}, e^{i\phi}) \mapsto (e^{i\phi}, e^{i\theta})$, which takes longitudes to meridians and meridians to longitudes.
- the meridional twist $(e^{i\theta}, e^{i\phi}) \mapsto (e^{i\theta+\phi}, e^{i\phi})$, shown in Figure 2.2.
- the longitudinal twist $(e^{i\theta}, e^{i\phi}) \mapsto (e^{i\theta}, e^{i\phi+\theta})$, also shown in Figure 2.2.

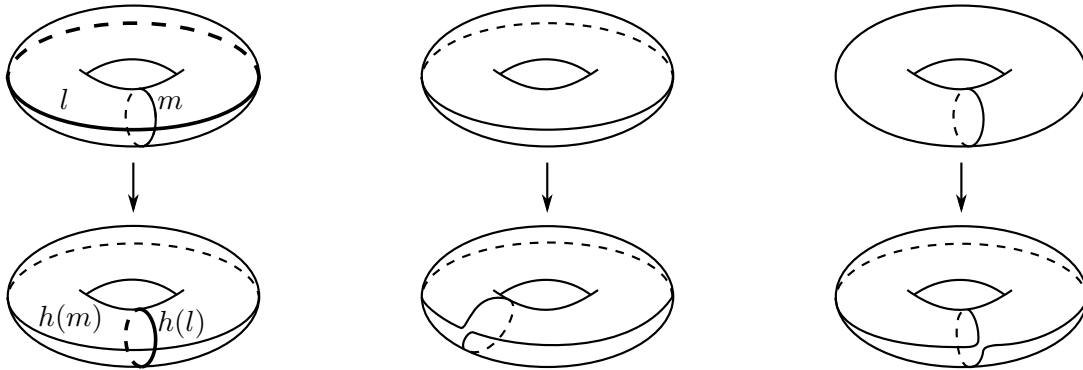


Figure 2.16: Three automorphisms of T^2 : the inversion (left), meridional twist (center) and longitudinal twist (right).

Tangle operations turn one tangle into another. So by the same process as we created torus knots from tangles, we can create automorphisms of the torus from tangle operations. In particular, H becomes the longitudinal twist (see Figure 2.2) and F becomes the inversion.

By the previous section, we know that elements of $H_1(T^2)$ have the form $\langle a, b \rangle$, where $m \in \langle 1, 0 \rangle$ and $l \in \langle 0, 1 \rangle$. So from any automorphism h of the torus, we get a group isomorphism

$$h_* : H_1(T^2) \rightarrow H_1(T^2), \text{ where } h_*(\langle a, b \rangle) = h_*(a\langle 1, 0 \rangle + b\langle 0, 1 \rangle) = a(h\langle 1, 0 \rangle) + b(h\langle 0, 1 \rangle).$$

To cast this in terms of $\text{GL}(2, \mathbb{Z})$, let $m = \begin{pmatrix} 1 \\ 0 \end{pmatrix}$ and $l = \begin{pmatrix} 0 \\ 1 \end{pmatrix}$. Then h_* will be the

$$\text{transformation } \begin{pmatrix} a & c \\ b & d \end{pmatrix}.$$

Since h is a homeomorphism, h^{-1} exists, and $(h^{-1})_* \circ h_* = \text{identity}$. Thus the matrix representing h is an invertible matrix, an element of $\text{GL}(2, \mathbb{Z})$.

Now we have defined the map $\Phi : \text{Aut}(T) \rightarrow \text{GL}(2, \mathbb{Z})$ that takes $h : T \rightarrow T$ to the matrix

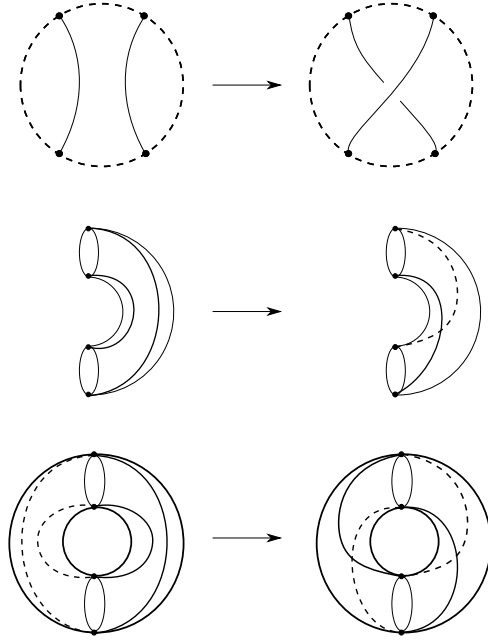


Figure 2.17: Three automorphisms of T^2 : the inversion (left), meridional twist (center) and longitudinal twist (right).

representing $h_* : H_1(T) \rightarrow H_1(T)$ in $\text{GL}(2, \mathbb{Z})$.

In particular,

- $\Phi(\text{longitudinal twist}) = \begin{pmatrix} 1 & 0 \\ 1 & 1 \end{pmatrix} := A$ (since a longitudinal twist maps the classes $\langle 1, 0 \rangle \mapsto \langle 1, 1 \rangle$ and $\langle 0, 1 \rangle \mapsto \langle 0, 1 \rangle$)
- $\Phi(\text{meridional twist}) = \begin{pmatrix} 1 & 1 \\ 0 & 1 \end{pmatrix} := B$
- $\Phi(\text{inversion}) = \begin{pmatrix} 0 & 1 \\ 1 & 0 \end{pmatrix} := C$

Noting that A, B and C generate $\text{GL}(2, \mathbb{Z})$, we have that Φ is surjective.

Next, consider the kernel of Φ .

Proposition 2.1. *Two automorphisms h and h' of T^2 are isotopic if and only if $\Phi(h) = \Phi(h')$.*

Proof. Suppose $h, h' \in \text{Aut}(T)$ are isotopic. Then the restriction of the isotopy between them to the meridian gives an isotopy between $h(m)$ and $h'(m)$. Then $[h(m) - h'(m)] = \langle 0, 0 \rangle \in H_1(T^2)$,

so $[h(m)] = [h'(m)] = \langle a, b \rangle \in H_1(T^2)$. Similarly, $[h(l)] = [h'(l)] = \langle c, d \rangle$. So

$$\Phi(h) = \begin{pmatrix} a & c \\ b & d \end{pmatrix} = \Phi(h')$$

Now, suppose $\Phi(h) = \Phi(h')$. Then $[h(m)] = \langle a, b \rangle = [h'(m)]$. By Theorem 2.1, then, $h(m)$ and $h'(m)$ are isotopic. So there is an isotopy $\phi_1 : [0, 1] \times m \rightarrow T^2$ such that $\phi_1(0, m) = h(m)$ and $\phi_1(1, m) = h'(m)$. Similarly, there is an isotopy $\phi_2 : [0, 1] \times l \rightarrow T^2$ such that $\phi_2(0, l) = h(l)$ and $\phi_2(1, l) = h'(l)$. We can extend this to an isotopy $\phi : [0, 1] \times T^2 \rightarrow T^2$ that restricts to ϕ_1 and ϕ_2 on the appropriate domains, and with $\phi(0, t) = h(t)$, $\phi(1, t) = h'(t)$ everywhere [20]. Thus h and h' are isotopic. \square

It follows that $\ker(\Phi) = \{h \in \text{Aut}(T^2) \mid h \text{ isotopic to the identity}\}$. By the first isomorphism theorem, $\text{Aut}(T^2)/\ker(\Phi) \cong \text{GL}(2, \mathbb{Z})$.

The covering map from the torus to the 4-point sphere transformed rational tangles into torus knots, and tangle operations into automorphisms of the torus. The discussion of the map Φ above relates torus knots to elements of $H_1(T^2)$, and automorphisms of the torus to elements of $\text{GL}(2, \mathbb{Z})$. With this in mind, we can rewrite Conway's algorithm so that instead of using tangle operations to produce rational tangles, it uses elements of $\text{GL}(2, \mathbb{Z})$ to produce elements of $H_1(T^2)$.

- Begin with $t := t_\infty$. Under the covering map, t_∞ corresponds to the longitude of the torus, which represents the element $\langle 0, 1 \rangle \in H_1(T^2)$. Abusing notation, write $\langle 0, 1 \rangle = \begin{pmatrix} 0 \\ 1 \end{pmatrix}$.
- For each i from n to 1, let $t := H^{a_i}(F(t))$. Under the covering map from the torus to the four-point sphere, H corresponds to a longitudinal twist. The image of the longitudinal twist (or any automorphism isotopic to it) under Φ is $\begin{pmatrix} 1 & 0 \\ 1 & 1 \end{pmatrix}$. Similarly, F is related to the inversion automorphism which corresponds to $\begin{pmatrix} 0 & 1 \\ 1 & 0 \end{pmatrix}$.

So we have (again abusing notation) $t := \begin{pmatrix} 1 & 1 \\ 0 & 1 \end{pmatrix}^{a_i} \begin{pmatrix} 0 & 1 \\ 1 & 0 \end{pmatrix} t$

For simplicity, define $M(n) = H^n F = \begin{pmatrix} 0 & 1 \\ 1 & n \end{pmatrix}$. The second step in the algorithm then

becomes $t := M(a_i)t$. So the final result of this algorithm is an element of $H_1(T^2)$ of the form $M(a_1)M(a_2)\dots M(a_n) \begin{pmatrix} 0 \\ 1 \end{pmatrix}$.

Next, we relate the algorithm to continued fractions.

Definition 27. A *continued fraction* is of the form

$$C(a_1, a_2, \dots, a_n) = a_1 + \frac{1}{a_2 + \frac{1}{a_3 + \frac{1}{\ddots + \frac{1}{a_n}}}}$$

for $a_1, a_2, \dots, a_n \in \mathbb{Z}$ and nonzero a_n .

Any rational number p/q can be expanded into the form of a continued fraction using the Euclidean algorithm as follows:

- Let $r_{-1} := p$, $r_0 := q$ and $i := -1$.
- Until $r_{i+1} = 0$, repeat:
- Let $i := i + 1$. Set a_{i+1}, r_{i+1} such that $r_{i-1} = a_{i+1}r_i + r_{i+1}$, and $0 \leq r_{i+1} < r_i$

The sequence of $\{a_i\}$ obtained by this process gives $C(a_1, \dots, a_n) = p/q$.

We can adapt the Euclidean algorithm, using matrix multiplication and the $M(n)$ defined above, to obtain an expression for the vector $\begin{pmatrix} q \\ p \end{pmatrix}$:

- Let $r_{-1} := p$, $r_0 := q$ and $i := -1$.
- Until $r_{i+1} = 0$, repeat:
- Let $i := i + 1$. Set a_{i+1}, r_{i+1} such that

$$M(a_{i+1}) \begin{pmatrix} r_i \\ r_{i+1} \end{pmatrix} = \begin{pmatrix} r_i \\ a_{i+1}r_i + r_{i+1} \end{pmatrix} = \begin{pmatrix} r_i \\ r_{i-1} \end{pmatrix} \text{ and } 0 \leq r_{i+1} < r_i.$$

The sequence of $M(a_i)$ obtained by this process gives $M(a_1)M(a_2)\dots M(a_n) \begin{pmatrix} 0 \\ 1 \end{pmatrix} = \begin{pmatrix} q \\ p \end{pmatrix}$.

Notice that the equality $a_{i+1}r_i + r_{i+1} = r_{i-1}$ given by the bottom entries in the equation of vectors in the third step of the new algorithm is precisely the condition of the last step in the original Euclidean algorithm. So the statements

$$C(a_1, \dots, a_n) = p/q \text{ and } M(a_1)M(a_2)\dots M(a_n) \begin{pmatrix} 0 \\ 1 \end{pmatrix} = \begin{pmatrix} q \\ p \end{pmatrix}$$

are equivalent.

Theorem 2.2 (Conway's Theorem). *Two rational tangles formed from Conway's algorithm using the integer sequences a_1, a_2, \dots, a_n and b_1, b_2, \dots, b_n are equivalent if and only if $C(a_1, a_2, \dots, a_n) = C(b_1, b_2, \dots, b_n)$.*

Proof. We know that two rational tangles (formed from integer sequences $\{a_i\}$ and $\{b_i\}$) are equivalent (isotopic) if and only if their associated elements of $H_1(T^2)$ are equal. Using the modified version of Conway's algorithm, this means that

$$M(a_1)M(a_2)\dots M(a_n) \begin{pmatrix} 0 \\ 1 \end{pmatrix} = M(b_1)M(b_2)\dots M(b_n) \begin{pmatrix} 0 \\ 1 \end{pmatrix}.$$

If $C(a_1, a_2, \dots, a_n) = C(b_1, b_2, \dots, b_n)$, then using the matrix form of the Euclidean algorithm, we know that

$$M(a_1)M(a_2)\dots M(a_n) \begin{pmatrix} 0 \\ 1 \end{pmatrix} = M(b_1)M(b_2)\dots M(b_n) \begin{pmatrix} 0 \\ 1 \end{pmatrix}.$$

These two conditions are equivalent, so the proof is finished. □

So we can associate a tangle formed from the sequence $\{a_i\}$ with the rational number $C(a_1, a_2, \dots, a_n) = p/q$, and call this tangle $t_{p/q}$. From Conway's theorem, we see that $t_{p/q}$ is the tangle that becomes the torus knot $T(p, q)$ under the covering map from the torus to the four-point sphere. This is the generalization of the labeling of $T(0, 1)$ as t_0 and $T(1, 0)$ as t_∞ .

Chapter 3

Heegaard Splittings

In Section 1.2.2, we described the complete classification of surfaces. In the case of 3-manifolds, the matter is more complicated. We will not reach a complete classification of 3-manifolds, but in the following chapters we'll see several ways of representing them, and classify some particular examples based on those representations. Heegaard splittings are one of these representations of 3-manifolds [10, 17, 20, 21]. In this chapter, we'll give examples of 3-manifolds obtained by Heegaard splittings. In particular, we'll discuss lens spaces, and show when two lens spaces are homeomorphic.

3.1 Definition

This section defines Heegaard splittings and describes several of their important properties.

Definition 28. A *Heegaard splitting* of a 3-manifold M is a triple (M_1, M_2, h) , where M_1 and M_2 are handlebodies, $h : \partial M_1 \rightarrow \partial M_2$ is a homeomorphism, and M is the resulting manifold when M_1 and M_2 are identified along their boundaries (glued together) by h .

Remark 6. M_1 and M_2 are homeomorphic. To see this, first notice that ∂M_1 and ∂M_2 are orientable surfaces. Since there is a homeomorphism between ∂M_1 and ∂M_2 , we know by the classification theorem for surfaces that they must have the same genus. Thus the solid handlebodies M_1 and M_2 must also be homeomorphic.

Remark 7. M has no boundary. Let $x \in \partial M_1$. Then $h(x) \in \partial M_2$. Since x and $h(x)$ are boundary points, they have neighborhoods U and U' , respectively, which are homeomorphic to \mathbb{R}_+^3 . The gluing of M_1 and M_2 performs the identification $x = h(x)$. So $x \in M$ has a

neighborhood $U \cup U'$ homeomorphic to \mathbb{R}^3 . Thus every point in the boundary of M_1 or M_2 maps to a point in the interior of M . Interior points of M_1 and M_2 are not affected by the gluing operation, so they remain interior points.

Remark 8. M is orientable. By the classification theorem for surfaces, ∂M_1 and ∂M_2 are orientable. Orient ∂M_1 , and choose a point $x \in \partial M_1$. Then assign $h(x) \in \partial M_2$ the orientation consistent with x . Given an orientation for a point in ∂M_2 , we can now orient all of ∂M_2 . Hence the orientations of ∂M_1 and ∂M_2 are consistent.

Given an orientation of ∂M_i (a choice of positive direction in each of 2 dimensions), there are two possible ways to consistently extend it to an orientation of M_i (we have a choice of positive direction in the third dimension). Making opposite choices for M_1 and M_2 yields a consistent orientation of M .

In fact, the conditions on M in Remarks 7 and 8 are sufficient for the existence of a Heegaard splitting:

Theorem 3.1. *Every orientable 3-manifold without boundary has a Heegaard splitting.*

Proof. Consider a triangulation K of M . (As a generalization of the 2-dimensional case given in Definition 12, we say K is a *triangulation* of a 3-manifold M if K is homeomorphic to M and $K = \bigcup_{i=1}^n T_i$, where T_i are tetrahedra which intersect pairwise at a vertex, along an entire edge or face, or nowhere. It can be shown that any manifold has a triangulation [16, 25].) It is sufficient to prove the theorem using a triangulation K of M , since the homeomorphism taking K to M transforms a Heegaard splitting of K into a Heegaard splitting of M .

Modify K in the following way. For every T_i , draw the three medians on each triangular face, subdividing the face into six triangles. Add a fourth vertex to each of these new triangles at the centroid of T_i , so that they become tetrahedra (see Figure 3.1). Now T_i is the union of 24 smaller tetrahedra.

Repeat this process (called *barycentric subdivision*) for each of the new tetrahedra. Hence each T_i is subdivided into 24^2 small tetrahedra.

Define subsets K_1 and K_2 of these small tetrahedra as follows. Let K_1 consist of all the small tetrahedra that intersect an edge of one of the T_i . Let K_2 contain those tetrahedra not in K_1 .

Next we show that K_1 and K_2 are homeomorphic handlebodies.

Consider $K_2 \cap T_i$. It takes the form of a ball in the center of T_i with four solid cylinders, one

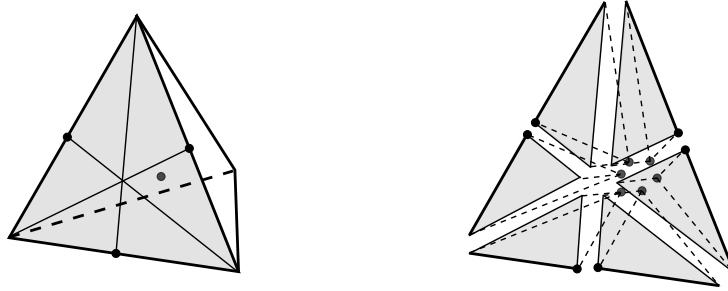


Figure 3.1: The six small tetrahedra adjacent to one face of a T_i after the first barycentric subdivision.

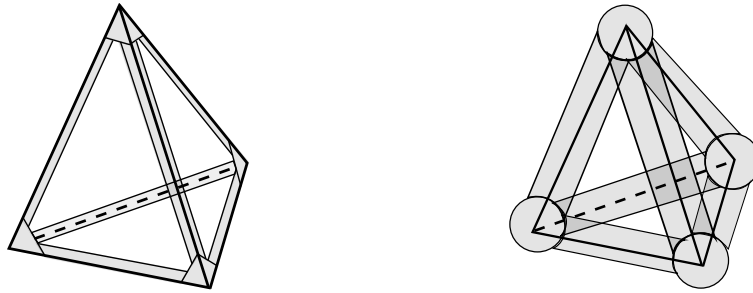


Figure 3.2: Left: the shaded region represents the intersection of T_i with K_1 . K_2 is the complement of the shaded region. Right: the ball-and-cylinder model of a portion of K_1 .

attaching the ball to each face of T_i . For adjacent T_i and T_j , the solids $K_2 \cap T_i$ and $K_2 \cap T_j$ are attached by the ends of these cylinders.

The ball-and-cylinder model can also be used to describe K_1 . In this case, the balls are located at the vertices of the T_i and the cylinders run along their edges, as shown on the right in Figure 3.1.

By induction, we show that any solid constructed out of balls and cylinders is a handlebody. This is sufficient to prove our claim, since then K_1 and K_2 are handlebodies with the same boundary, so they must be homeomorphic.

Define the induction step to be adding a solid cylinder by attaching each end to a ball. (Note that gluing a ball to a handlebody always yields a homeomorphic handlebody: since it doesn't change the genus or orientability of the boundary, it produces a manifold with boundary homeomorphic to the original. Since all ball-and-cylinder constructions are applications of the induction step and adding balls, proving that the induction step always yields a handlebody is sufficient to prove our claim.) Suppose the two ends of a cylinder are attached to the same handlebody. The boundary of the resulting manifold is still a surface; we must check that it is an orientable

one. Suppose not. Then K is nonorientable, which contradicts assumption. If the two ends of a cylinder are attached to two disjoint handlebodies, then we have no difficulty, since each is independently orientable. \square

3.2 Examples

Next we give some examples of Heegaard splittings.

Example 15 (A Heegaard splitting of the 3-sphere). A 3-sphere, as we have seen in Example 8, can be described as a subset of \mathbb{C}^2 : $S^3 = \{(ae^{i\alpha}, be^{i\beta}) \in \mathbb{C}^2 \mid a^2 + b^2 = 2\}$. Split S^3 into M_1 and M_2 as follows: $M_1 = \{(ae^{i\alpha}, be^{i\beta}) \in S^3 \mid a \leq b\}$, and $M_2 = \{(ae^{i\alpha}, be^{i\beta}) \in S^3 \mid a \geq b\}$. This means that $\partial M_1 = \partial M_2 = \{(e^{i\alpha}, e^{i\beta}) \in \mathbb{C}^2\}$, a 2-dimensional torus.

Claim: M_1 and M_2 are solid tori.

First, extend the coordinate system $(e^{i\theta}, e^{i\phi})$ for the 2-dimensional torus to coordinates $(e^{i\theta}, e^{i\phi}, r)$ for any point in a solid torus V , as shown:

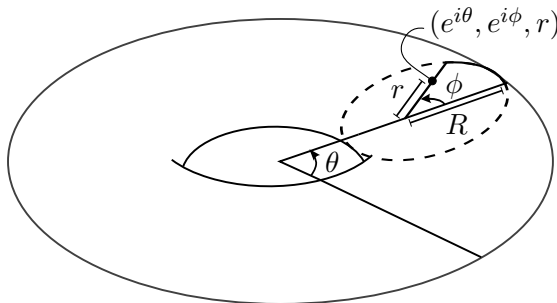


Figure 3.3: A coordinate system for the solid torus V .

As before, $\theta, \phi \in [0, 2\pi]$. Additionally, $0 \leq r \leq R$, where R is the radius of the tube of V , as shown above.

Since $a^2 + b^2 = 2$ for all $(ae^{i\alpha}, be^{i\beta}) \in S^3$, the condition $a \leq b$ in M_1 is equivalent to $a \leq 1$. So we have $M_1 = \{(ae^{i\alpha}, be^{i\beta}) \in S^3 \mid a \leq 1\} = \{(ae^{i\alpha}, \pm(\sqrt{2-a^2})e^{i\beta}) \mid a \leq 1\}$. Then there is a homeomorphism $h_1 : M_1 \rightarrow V$ with $h_1(ae^{i\alpha}, \pm(\sqrt{2-a^2})e^{i\beta}) = (e^{i\beta}, e^{i\alpha}, a)$.

In the same way, $M_2 = \{(\pm(\sqrt{2-b^2})e^{i\alpha}, be^{i\beta}) \mid b \leq 1\}$ also describes a solid torus, by the homeomorphism $h_2(\pm(\sqrt{2-b^2})e^{i\alpha}, be^{i\beta}) = (e^{i\alpha}, e^{i\beta}, b)$.

Let the homeomorphism $h : \partial M_1 \rightarrow \partial M_2$ be the restriction of $h_2^{-1} \circ h_1$ to ∂M_1 . We can get an

idea of how h glues M_1 and M_2 by looking at the images of meridians and longitudes of ∂M_1 under h . A meridian of ∂M_1 can be written $m_\beta = \{(e^{i\alpha}, e^{i\beta}) | 0 \leq \alpha \leq 2\pi\}$ for a fixed β . Then,

$$h(m_\beta) = h_2^{-1}\{(e^{i\beta}, e^{i\alpha}, 1) | 0 \leq \alpha \leq 2\pi\} = \{(e^{i\beta}, e^{i\alpha}) | 0 \leq \alpha \leq 2\pi\} \subset \partial M_2.$$

This describes a longitude of M_2 . Similarly, h maps longitudes of ∂M_1 to meridians of ∂M_2 .

A gluing of two tori in S^3 that takes longitudes to meridians and meridians to longitudes looks like this:

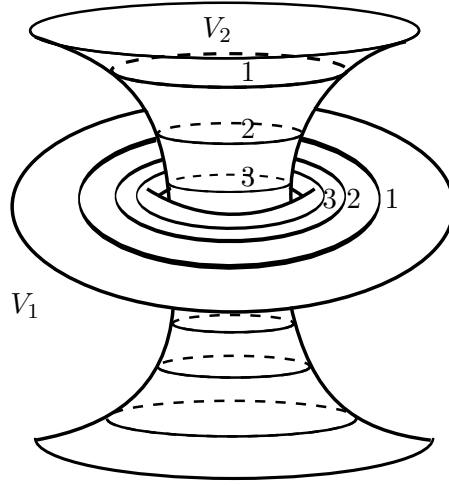


Figure 3.4: A Heegaard splitting $S^3 = (V_1, V_2, h)$. V_1 is visibly a solid torus, and V_2 is a solid torus (shown as a cylinder whose ends meet at the point at infinity). The homeomorphism h maps the longitudes shown on V_1 to meridians shown on V_2 .

In fact, there are Heegaard splittings of S^3 into two handlebodies of any genus g , which look like this:

Example 16. More generally, from a Heegaard splitting of any M^3 into two handlebodies M_1 and M_2 of genus g , we can obtain a Heegaard splitting of M^3 into two handlebodies of genus $g + 1$ through a process called *stabilization* [21], as follows. Add an unknotted handle H to M_1 , and call this new genus- $(g + 1)$ handlebody M'_1 . Let D be a disk such that $D \cap M'_1 = \partial D$, and ∂D is a longitude in M'_1 , as shown in Figure 16.

Let $C = D \times I$. Then $C \cup H$ is a 3-ball, and $M_2 \cup C$ is a $(g + 1)$ -handlebody, which we call M'_2 . So $M^3 = M_1 \cup M_2 \cong M_1 \cup M_2 \cup (C \cup H) \cong (M_1 \cup H) \cup (M_2 \cup C) \cong M'_1 \cup M'_2$, and we have created a Heegaard splitting of M^3 into two $(g + 1)$ -handlebodies.

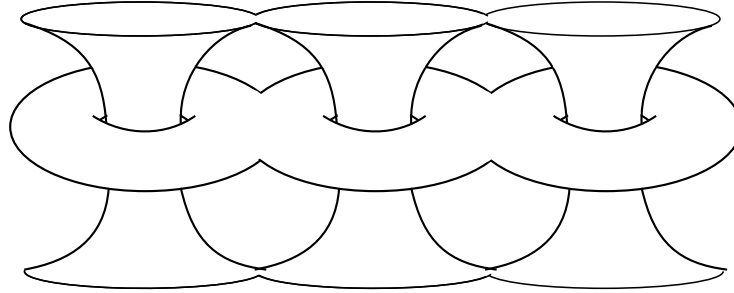


Figure 3.5: A Heegaard splitting $S^3 = (V_1, V_2, h)$. V_1 is visibly a solid torus, and V_2 is a solid cylinder whose ends meet at the point at infinity. The homeomorphism h maps the longitudes shown on V_1 to meridians shown on V_2 .

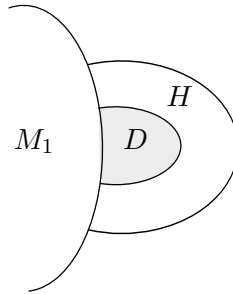


Figure 3.6: Adding a handle to M_1 in a Heegaard splitting.

Example 17 (Lens Spaces). We've seen a homeomorphism that glues two tori together to create a 3-sphere (Example 15). We now describe a class of homeomorphisms that glue tori to create lens spaces. Let $L(p, q)$, the (p, q) -lens space, be the manifold represented by the Heegaard splitting (M_1, M_2, h) , where M_1 and M_2 are solid tori and $h_* : H_1(\partial M_1) \rightarrow H_1(\partial M_2)$ maps $\langle 1, 0 \rangle$ to $\langle q, p \rangle$. Example 15 demonstrates that $L(1, 0) = S^3$.

A lens space can also be represented as a quotient space of S^3 . We will show that the two definitions are equivalent by demonstrating that this quotient space has exactly the Heegaard splitting described above. The quotient space is defined as follows: for coprime $p, q \in \mathbb{Z}_+$, let $\sigma_{p,q} : S^3 \rightarrow S^3$ be the map $\sigma_{p,q}(z, w) = (ze^{2\pi i/p}, we^{2\pi iq/p})$. Define an equivalence relation on points of S^3 such that $s_1 \sim s_2$ if and only if $s_1 = \sigma_{p,q}^n(s_2)$ for some $n \in \mathbb{Z}_+$. (Note that $(\sigma_{p,q})^p = \text{id}|_{S^3}$, so $(\sigma_{p,q}^n)^{-1} = \sigma_{p,q}^{p-n}$, and \sim is symmetric.)

Next use the Heegaard splitting of a 3-sphere into solid tori to obtain a Heegaard splitting of the quotient just defined, and show that this Heegaard splitting gives $L(p, q)$. First, consider the presentation of S^3 as (M_1, M_2, h) .

Lemma 3.1. $M_1^* := M_1/\sim$ and $M_2^* := M_2/\sim$ are solid tori.

Proof. First decompose $S^3 = \{(ae^{i\alpha}, be^{i\beta}) \in \mathbb{C}^2 \mid b = \sqrt{2 - a^2}\}$ into cells of dimension 0, 1, 2 and 3. There will be one cell of each dimension $0 \leq n \leq 3$ for each value of k in $0, 1, \dots, p-1$, as follows:

- 0-dimensional cell C_k^0 : $\{(0, e^{2\pi ik/p})\}$
- 1-dimensional cell C_k^1 : $\{(0, e^{2\pi i\theta}) \mid k/p \leq \theta \leq (k+1)/p\}$
- 2-dimensional cell C_k^2 : $\{(ae^{2\pi ik/p}, w) \mid 0 < a \leq 2\}$
- 3-dimensional cell C_k^3 : $\{(ae^{2\pi i\theta}, w) \mid 0 < a \leq 2, k/p \leq \theta \leq (k+1)/p\}$

Observe that σ permutes these cells: $\sigma(C_k^n) = C_{k+q}^n$. So, taking the quotient by \sim of the cellular decomposition gives four elements: $\{\sigma^k(C_1^0) \mid k = 0, 1, \dots, p-1\}$, $\{\sigma^k(C_1^1) \mid k = 0, 1, \dots, p-1\}$, $\{\sigma^k(C_1^2) \mid k = 0, 1, \dots, p-1\}$ and $\{\sigma^k(C_1^3) \mid k = 0, 1, \dots, p-1\}$. Thus obtain a presentation of S^3/\sim as the union of one representative cell from each dimension. Since the $C_k^0, C_k^1, C_k^2 \in \partial C_k^3$, this space is really C_k^3 , with gluing of the boundary as given by σ . We call this space S^* .

The next goal is to describe M_1^* and M_2^* as subsets of S^* . To make it easier to visualize, first perform a change of coordinates. Define $f : S^3 \rightarrow \mathbb{R}^3$ by

$$f(ae^{2\pi i\alpha}, be^{2\pi i\beta}) = (b \cos 2\pi\beta, b \sin 2\pi\beta, a(2p\alpha - 2k - 1)) = (x_1, x_2, x_3).$$

Note that $\frac{k}{p} \leq \alpha \leq \frac{k+1}{p}$ for all $(ae^{2\pi i\alpha}, be^{2\pi i\beta}) \in S^*$, so

$$2p\alpha - 2k - 1 \leq 1 \text{ and } |x_3| = a|2p\alpha - 2k - 1| \leq a.$$

Also,

$$x_1^2 + x_2^2 = b^2(\cos^2(2\pi\beta) + \sin^2(2\pi\beta)) = b^2.$$

So $x_1^2 + x_2^2 + x_3^2 \leq a^2 + b^2 \leq 2$, which means that $f(S^*)$ is the ball of radius 2 in \mathbb{R}^3 . When $\alpha = k/p$, the point $(ae^{2\pi i\alpha}, be^{2\pi i\beta})$ maps to a point on the boundary of this ball, with $x_3 < 0$. And when $\alpha = (k+1)/p$, $(ae^{2\pi i\alpha}, be^{2\pi i\beta})$ maps to a point on the boundary with $x_3 > 0$. We represent $f(S^*)$ as a slightly flattened (or lens-shaped) ball in \mathbb{R}^3 (see Figure 17).

Since we know which points in S^* map to the boundary of the lens in \mathbb{R}^3 , we can use σ to perform the proper identifications. Suppose $\alpha = k/p$. Then $\sigma(ae^{2\pi i\alpha}, be^{2\pi i\beta}) = (ae^{2\pi i(\frac{k+1}{p})}, be^{2\pi i(\beta + \frac{q}{p})})$, which is a point on the boundary sphere with $x_3 > 0$ and rotated in the x_1x_2 -plane by $2\pi q/p$.

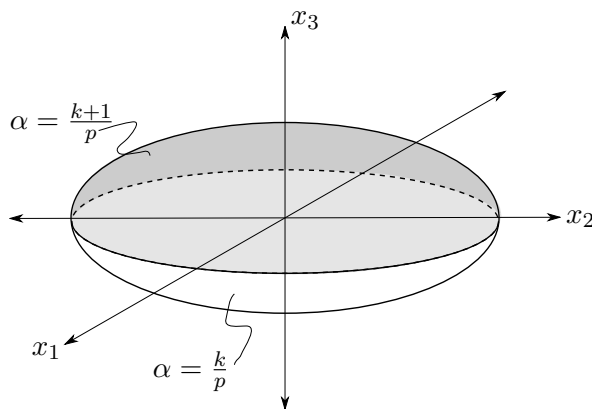


Figure 3.7: The lens S^* . Its boundary consists of the points $(ae^{2\pi i\alpha}, be^{2\pi i\beta}) \in S^*$ with $\alpha = \frac{k}{p}$ or $\alpha = \frac{k+1}{p}$.

So S^* is represented by a lens in \mathbb{R}^3 , with the top and bottom boundary components identified after a $2\pi q/p$ twist.

We can finally find M_1^* and M_2^* , pictured in Figure 17. Recall that

$$M_1 = \{(ae^{2\pi i\alpha}, be^{2\pi i\beta}) \in S^3 \mid |a| \leq 1\}, \text{ and } M_2 = \{(ae^{2\pi i\alpha}, be^{2\pi i\beta}) \in S^3 \mid 1 \leq |a| \leq 2\}.$$

So, in the lens, M_2^* is the set of points with $x_1^2 + x_2^2 \leq 1$: that is, the “core” of radius 1 in the lens. Adding boundary identifications, the top and bottom caps of the core are glued together with a twist of $2\pi q/p$, to form a solid torus. M_1^* is the set points in the lens with $x_1^2 + x_2^2 \geq 1$. In Theorem 3.2, we will see how the boundary identifications make this a solid torus. \square

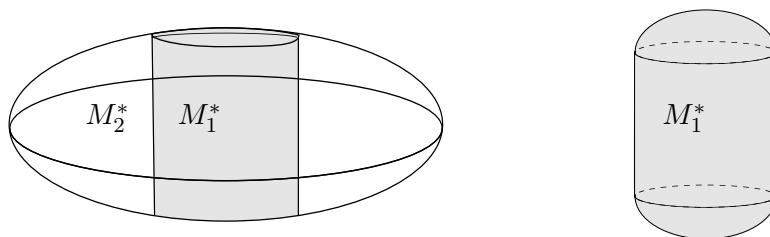


Figure 3.8: A Heegaard splitting of the lens into M_1^* and M_2^* .

Now, to obtain a lens space from M_1^* and M_2^* , glue them back together under the original identifications from the Heegaard splitting of S^3 . What does this homeomorphism look like on the new solid tori? $h_* : H_1(\partial M_1) \rightarrow H_1(\partial M_2)$ maps $\langle 1, 0 \rangle$ to $\langle q, p \rangle$. Thus h , together with two solid tori, describes a Heegaard splitting of the lens space.

Theorem 3.2. *If $qq' \equiv \pm 1 \pmod{p}$, then $L(p, q) \cong L(p, q')$.*

Proof. We begin with the representation of $L(p, q)$ as the lens described above. First, divide the lens into p tetrahedra all meeting at the center (see Figure 3.2, left). Label the tetrahedra $1, 2, \dots, p$, with the index increasing as we move clockwise. Additionally, label the faces of each tetrahedron. The inner faces are A_i and B_i , where A_i is adjacent to $B_{i+1 \pmod{p}}$. Label the top faces T_i and the bottom faces S_i . Let the resulting representation of $L(p, q)$ be called L_1 .

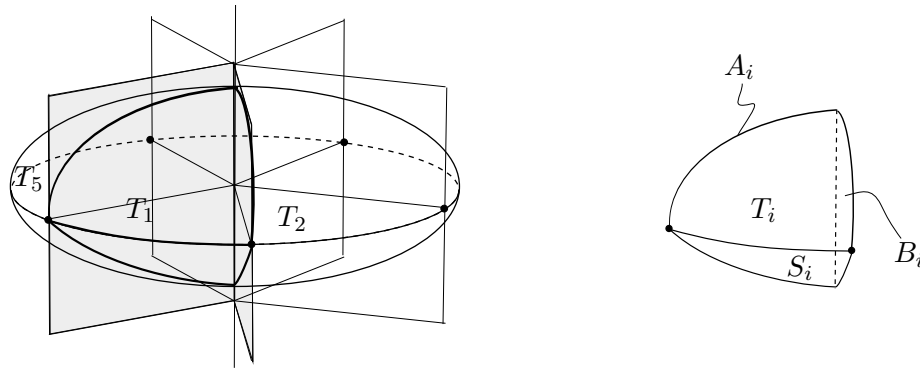


Figure 3.9: The division of a lens into tetrahedra (left) and the labeled faces of one tetrahedron (right).

The identifications of the boundary of L_1 , as discussed in the previous example, glue together the T and S faces of the tetrahedra: in particular, T_i is identified with $S_{i+q \pmod{p}}$. Cutting along the A and B faces and gluing instead along the S and T 's, we create a new, but equivalent, representation of $L(p, q)$, called L_2 :

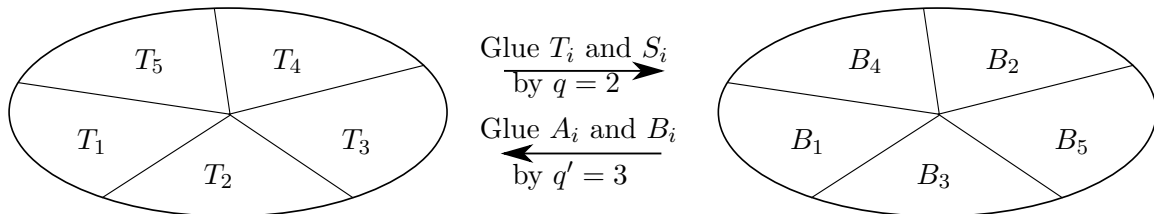


Figure 3.10: An overhead view of the division of a lens into tetrahedra, demonstrating that $L(5, 2) \cong L(5, 3)$.

As we move clockwise, the indices of the tetrahedra now increase by q : that is, they are encountered in the order $q, 2q, \dots, pq \equiv q$.

Next, re-identify the A and B faces, but this time to create $L(p, q')$. Each A_i is glued to the B

face of the tetrahedron q' clockwise steps away in L_2 . That is, A_i is identified with $B_{i+q'q}$. But $q'q \equiv 1 \pmod{p}$ means that $B_{i+q'q} = B_{i+1}$. Thus A_i is identified with B_{i+1} , and this gluing yields $L(p, q)$. And since, by definition, the gluing also creates $L(p, q')$, we have the desired fact that $L(p, q)$ and $L(p, q')$ are homeomorphic. \square

Chapter 4

Dehn Twists: Homeomorphisms of 2- and 3-Manifolds

All homeomorphisms of 2-manifolds can be written in terms of a specific class of homeomorphisms called Dehn twists. Although Dehn twists cannot be generally defined on 3-manifolds, some of them provide a way of constructing homeomorphisms of 3-manifolds. We focus on the solid torus as an example of homeomorphisms on 3-manifolds.

4.1 2-Manifolds

We first consider homeomorphisms of 2-manifolds. In particular, we define a Dehn twist, and then show that any homeomorphism of a 2-manifold can be written in terms of Dehn twists.

Definition 29. Let S be a 2-manifold, and γ a nonseparating curve in S . The following homeomorphism of S , illustrated in Figure 4.1, is called a *Dehn twist*:

- Cut S along γ , so that S has two copies of γ as boundary components.
- Fix one copy of γ . Rotate the other copy by 2π , and move points in a neighborhood of it so that the function is continuous.
- Reglue the two copies of γ .

Example 18. Since Dehn twists of the torus are homeomorphisms, we know from Chapter 2 that

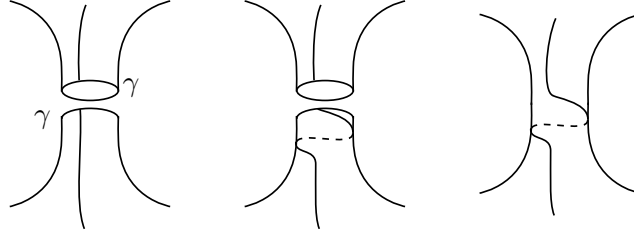


Figure 4.1: A Dehn twist along a curve γ in a surface S .

they can be represented as elements of $\text{GL}(2, \mathbb{Z})$. In particular, if the curve γ is a meridian, the homeomorphism is of the form $\begin{pmatrix} 1 & 1 \\ 0 & 1 \end{pmatrix}$, since meridians are mapped to $\langle 1, 0 \rangle$ and longitudes to $\langle 1, 1 \rangle$. Note that this homeomorphism appeared in Section 2.2 as the meridional twist (see Figure 2.2, center).

If γ is a longitude, the Dehn twist is the longitudinal twist from Section 2.2, represented by $\begin{pmatrix} 1 & 0 \\ 1 & 1 \end{pmatrix}$ (see Figure 2.2, right).

Definition 30. A homeomorphism h of a surface is called a *C-homeomorphism* if it is a composition of Dehn twists and homeomorphisms isotopic to the identity. If a C-homeomorphism between two spaces X and Y exists, write $X \sim_C Y$. (It can easily be checked that this is an equivalence relation.)

In fact, C-homeomorphisms completely describe the homeomorphisms of surfaces:

Theorem 4.1 (Dehn-Lickorish Theorem). *Let M^2 be a compact, orientable 2-manifold without boundary. All orientation-preserving homeomorphisms of M^2 are C-homeomorphisms.*

The following proof is based on the one found in [17]. For the original, see [14].

Proof. Note that the conditions on M^2 , together with the classification theorem for surfaces, imply that M^2 is a g -handlebody.

This proof requires the following lemma.

Lemma 4.1. *Suppose γ_1 and γ_2 are closed, nonseparating curves in M^2 . Then there exists a C-homeomorphism taking γ_1 to γ_2 .*

Proof. We will divide the proof into three cases:

Case 1: γ_1 and γ_2 have a single, transverse intersection point. Define τ_γ to be a Dehn twist along γ . Then, as the following figure demonstrates, $\tau_{\gamma_1} \circ \tau_{\gamma_2}(\gamma_1)$ is isotopic to γ_2 .

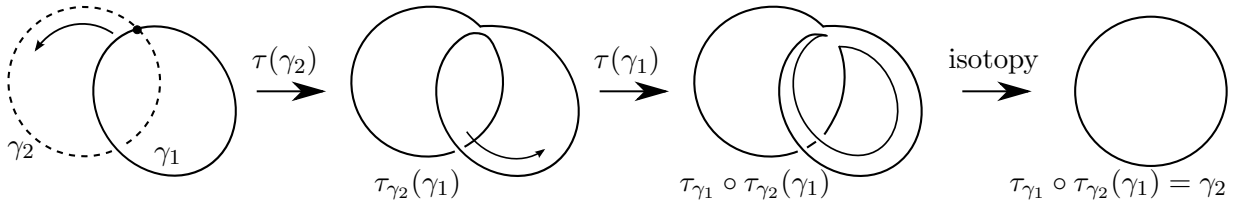


Figure 4.2: A homeomorphism of S taking γ_1 to γ_2 .

Case 2: $\gamma_1 \cap \gamma_2 = \emptyset$. Define a curve α that does not disconnect M^2 , and that intersects each of γ_1 and γ_2 once, transversely. (Then, by application of Case 1, we will have that $\gamma_1 \sim_C \alpha \sim_C \gamma_2$, so $\gamma_1 \sim_C \gamma_2$.) Suppose $\gamma_1 \cup \gamma_2$ disconnects S . Then γ_1 and γ_2 encircle the same handle of M^2 as shown below. Then let α be the curve in Figure 4.1(A).

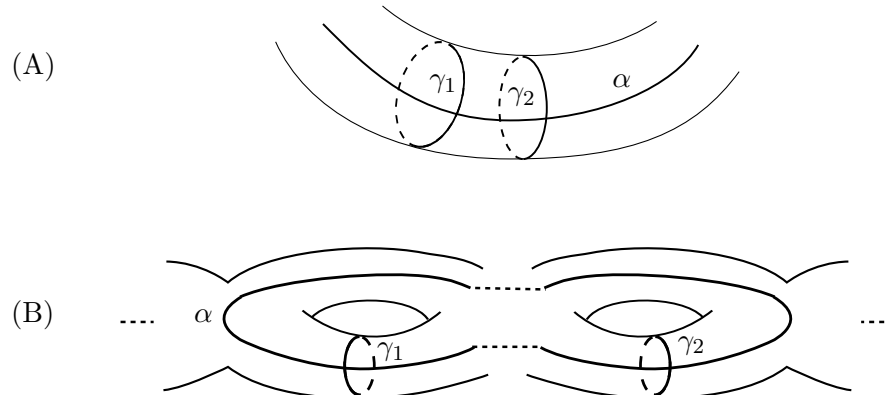


Figure 4.3: Curves α that do not disconnect M^2 , and that intersect γ_1 and γ_2 each once, transversely.

Now suppose γ_1 and γ_2 do not disconnect S . Then γ_1 and γ_2 encircle different handles of the same handlebody, and Figure 4.1(B) shows the placement of an appropriate α .

Case 3: γ_1 and γ_2 intersect more than once. We can assume that there are a finite number (n) of intersections of γ_1 and γ_2 , all transverse, since this situation can always be achieved by small perturbations (isotopies) of γ_1 and γ_2 . To show $\gamma_1 \sim_C \gamma_2$, find a curve α that does not disconnect S , and that intersects γ_1 no more than once and γ_2 fewer than n times. Then, by Cases 1 and 2, $\gamma_1 \sim_C \alpha$. By repeated application, obtain a curve C-homeomorphic to γ_1 that intersects γ_2 no more than once, and use Case 1 or 2 to conclude.

Now we find α . Consider two points x and y in $\gamma_1 \cap \gamma_2$, such that there are no other intersection points of γ_1 and γ_2 between x and y on γ_2 . Let l be the arc between x and y in γ_2 , and let the two components of $\gamma_1 \setminus \{x, y\}$ be β_1 and β_2 .

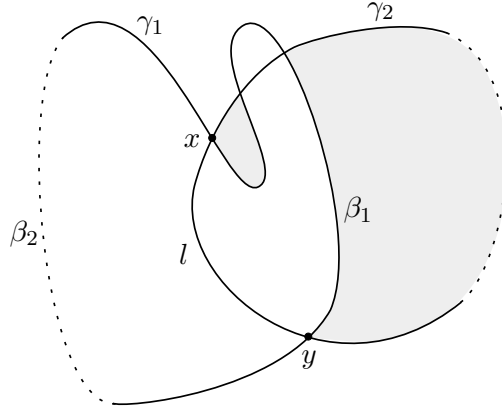


Figure 4.4: For this γ_1 and γ_2 , either $l \cup \beta_1$ or $l \cup \beta_2$ is the required α .

Either $\alpha_1 = \beta_1 \cup l$ or $\alpha_2 = \beta_2 \cup l$ does not disconnect M^2 . If both α_1 and α_2 disconnect M^2 , then no path exists to the shaded region of Figure 4.1 from the interior of α_1 or from the interior of α_2 . But $\text{int}(\gamma_1) = \text{int}(\alpha_1) \cup \text{int}(\alpha_2)$, so there is no path from $\text{int}(\gamma_1)$ to the shaded region, contradicting the fact that γ_1 does not disconnect M^2 .

Suppose without loss of generality that α_1 does not disconnect M^2 . Then, by a small perturbation, α_1 can be changed into the required α . \square

Since M^2 is a g -handlebody, we can cut along g meridians m_1, m_2, \dots, m_g of M^2 to obtain a disk with $2g$ boundary components ($2g - 1$ punctures). Let an ϵ -neighborhood of m_i be divided into two pieces U_i and U'_i , separated by m_i . Consider the effect of a homeomorphism $h : M^2 \rightarrow M^2$ on this punctured disk.

Since h is a homeomorphism and m_1 doesn't disconnect M^2 , $h(m_1)$ doesn't disconnect M^2 . So, by Lemma 4.1, there exists a C -homeomorphism f_1 such that $f_1(h(m_1)) = m_1$.

Suppose $f_1 \circ h$ is orientation-preserving. Then there exists a homeomorphism f'_1 isotopic to f_1 such that $(f'_1 \circ h)|_{m_1} = \text{id}|_{m_1}$ and $f'_1 \circ h$ maps U_1 (resp. U'_1) to the interior of U_1 (resp. U'_1). Thus $f'_1 \circ h$ is a homeomorphism of M^2 cut along m_1 , and it is the identity along the boundary. Repeat this process for each m_i , to obtain a homeomorphism $f'_g \circ \dots \circ f'_1 \circ h$ defined on the disk with $g - 1$ punctures which is the identity on the boundary. Then $f'_g \circ \dots \circ f'_1 \circ h$ is a C -homeomorphism (see [17]), so h must be a C -homeomorphism.

If $f_1 \circ h$ is not orientation-preserving, then we write $f_1 \circ h(m_1) = m_1^{-1}$, where m_1^{-1} contains the same points as m_1 but has opposite orientation. Construct a homeomorphism f_1^* of M^2 such that $f_1^*(h(m_1)) = m_1$ as follows. Because m_1 is a meridian of a handlebody, there exists a curve γ that intersects m_1 exactly once. The homeomorphism $(\tau_\gamma \circ \tau_{m_1} \circ \tau_\gamma)^2$ of M^2 takes m_1 to m_1^{-1} and γ to γ^{-1} . Let $f_1^* = (\tau_\gamma \circ \tau_{m_1} \circ \tau_\gamma)^2 \circ f_1$. Then

$$f_1^* \circ h(m_1) = (\tau_\gamma \circ \tau_{m_1} \circ \tau_\gamma)^2 \circ f_1 \circ h(m_1) = (\tau_\gamma \circ \tau_{m_1} \circ \tau_\gamma)^2(m_1^{-1}) = m_1,$$

as desired. Now the argument from the orientation-preserving case applies. \square

4.2 3-Manifolds

Although Dehn twists are defined for surfaces, the definition can be partially extended to homeomorphisms of 3-manifolds. We demonstrate this using the example of the solid torus. In general, using Theorem 4.1, we obtain a procedure for creating homeomorphisms of 3-manifolds from homeomorphisms of their boundaries by removing solid tori. The ideas developed in this section are necessary background for the surgery techniques of Chapter 5.

4.2.1 Homeomorphisms of the solid torus

In this subsection, we discuss the solid torus $V = D^2 \times S^1$. As with the torus as a surface ($T^2 = S^1 \times S^1$), we can define the meridian and longitude of V . We will see which Dehn twists of T^2 can be generalized to the solid torus. Finally, we will note how automorphisms of the solid torus change embedded knots. This information is used later in the proof of Theorem 5.1. The following can be found in [20].

Definition 31. A *meridian* of V is a simple, closed curve $m \subset \partial V$ that bounds a disk in V , but not in ∂V .

Remark 9. Equivalently, a meridian is a simple, closed curve in ∂V that is trivial in $\pi_1(V)$ and $H_1(V)$, but not in $\pi_1(\partial V)$ and $H_1(\partial V)$.

Figure 4.2.1 shows some examples and counterexamples of meridians of the solid torus:

Observe that all meridians of a solid torus V are representatives of the torus knot type $\langle 1, 0 \rangle \in H_1(\partial V)$. Thus, by Theorem 2.1, all meridians of V are ambient isotopic in ∂V (and in V).

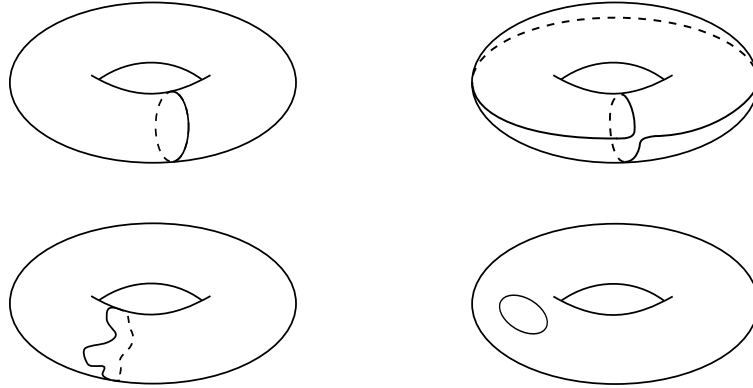


Figure 4.5: The curves at left are meridians of the solid torus. The ones at right are not.

Definition 32. A simple, closed curve l in ∂V is a *longitude* of V if there exists a meridian m of V such that l and m intersect once, and the intersection is transverse.

Remark 10. Equivalently, a longitude is a simple, closed curve in ∂V that represents the generator of $\pi_1(V)$ and $H_1(V)$.

There are infinitely many non-ambient isotopic longitudes. Here are some examples (at top) and counterexamples (at bottom):

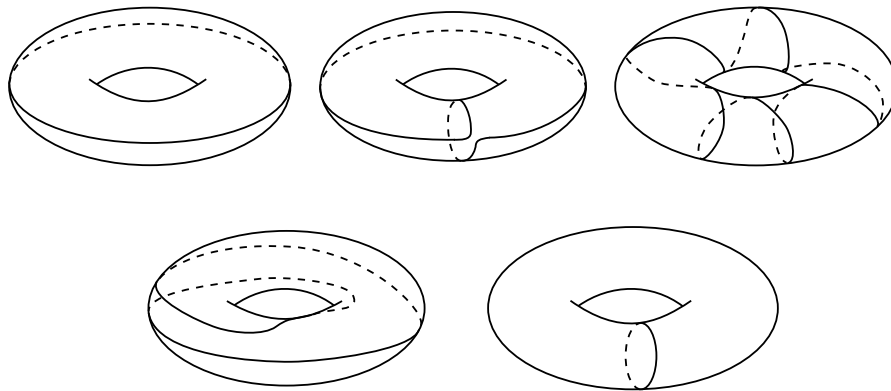


Figure 4.6: The curves at top are longitudes of the solid torus. The ones at bottom are not.

All homeomorphisms of V are isotopic to the solid torus version of meridional Dehn twists:

Proposition 4.1. A homeomorphism h of ∂V extends to a homeomorphism f of V if and only if it takes meridians to meridians.

Proof. By Theorem 4.1, we can assume any homeomorphism h of ∂V is a C-homeomorphism.

First, we assume $h : \partial V \rightarrow \partial V$ takes meridians to meridians and show that it must extend to

all of V . By Theorem 4.1, h must be a composition of meridional twists and homeomorphisms isotopic to the identity. Assume h is a single meridional twist along the meridian γ . To create f , instead of slicing ∂V along γ , slice V along the plane containing γ to get a solid cylinder. Perform a full twist on one base of the cylinder, also twisting a neighborhood of it to maintain continuity. Each point on the base, rotated by 2π , is returned to its original position. So we can glue the bases together again and get a homeomorphism.

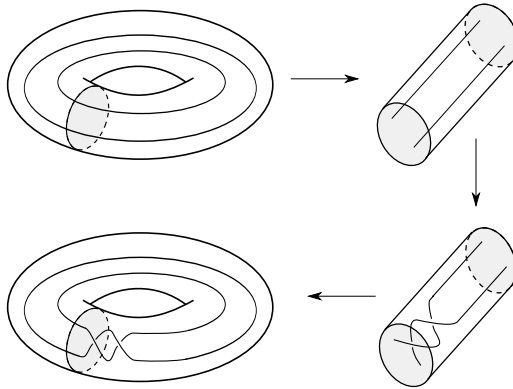


Figure 4.7: A homeomorphism of a solid torus extended from a homeomorphism of its boundary.

Now suppose h is a composition of meridional twists and homeomorphisms isotopic to the identity. We've shown that each meridional twist extends to a homeomorphism of V (and a homeomorphism of ∂V isotopic to the identity must extend to V), so the composition h also extends to a homeomorphism of V .

Suppose h is a homeomorphism of ∂V that extends to a homeomorphism f of V , and h doesn't take meridians to meridians. Then $h(\langle 1, 0 \rangle) = \langle m, n \rangle$, where $m, n \in \mathbb{Z}$ and $n \neq 0$. This means that the image of a meridian of V under f is a longitude in V .

Let γ_0 be a meridian of V such that $\gamma_0 = \{(1, \theta, \phi) \in V \mid 0 \leq \phi \leq 2\pi\}$ for a fixed θ . Now define $\gamma_t = \{(1-t, \theta, \phi) \in V \mid 0 \leq \phi \leq 2\pi\}$ for $0 \leq t \leq 1$.

The curves γ_0 and γ_1 are homotopic in V . Since f is a homeomorphism, it must be continuous as a function of r , so $f \circ \gamma_t$ is continuous as t varies. Thus $f \circ \gamma_0$ and $f \circ \gamma_1$ are homotopic.

But since γ_0 is a meridian of V , $f(\gamma_0)$ is a longitude of V , which means it is a generator of $\pi_1(V)$. And $f(\gamma_1) = p$ for some point $p \in V$, and this is trivial in $\pi_1(V)$. So, by contradiction, h must take meridians to meridians. \square

Homeomorphisms transform one ambient isotopy class of longitude into another. However,

for a given solid torus V , there is one ambient isotopy class of *preferred longitude*: the class represented by longitudes that have linking number zero with the core of the V . (Equivalently, if V is embedded in S^3 , the preferred longitude is the one that is trivial in $H_1(S^3 \setminus V)$.)

As we can see in Figure 4.2.1, the appearance of the preferred longitude depends on the embedding of V .

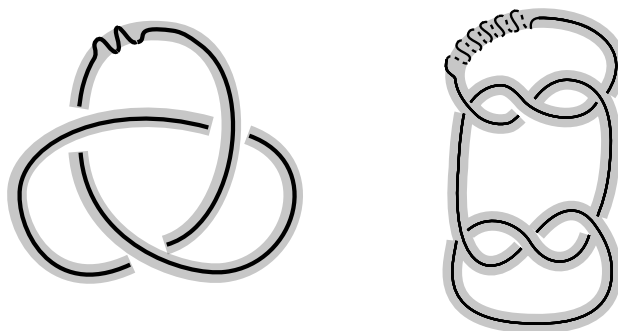


Figure 4.8: Preferred longitudes of two solid tori embedded in S^3 .

A homeomorphism of a 3-manifold may change embedded links, that is, nonisotopic links can have homeomorphic complements. In particular, there exist homeomorphisms of the solid torus that change embedded knots.

Proposition 4.2. *Let V be a solid torus, D a 3-disk and $V \subset D \subset \mathbb{R}^3$. There exists a homeomorphism $h : (\mathbb{R}^3 \setminus V) \rightarrow (\mathbb{R}^3 \setminus V)$ which is the identity outside of D , and switches the value of a crossing in $D \setminus V$ as shown below:*

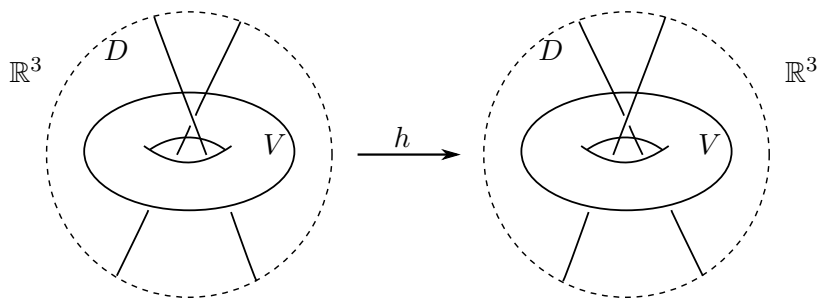


Figure 4.9: The homeomorphism h of $\mathbb{R}^3 \setminus V$ changes the crossing as shown, and is the identity outside of D .

Proof. Construct h as follows. Cut the section of D that passes through the hole of V with a plane containing a preferred longitude of V , as shown.

A twist of 2π along this cut is a homeomorphism of $D \setminus V$, which interchanges the crossing

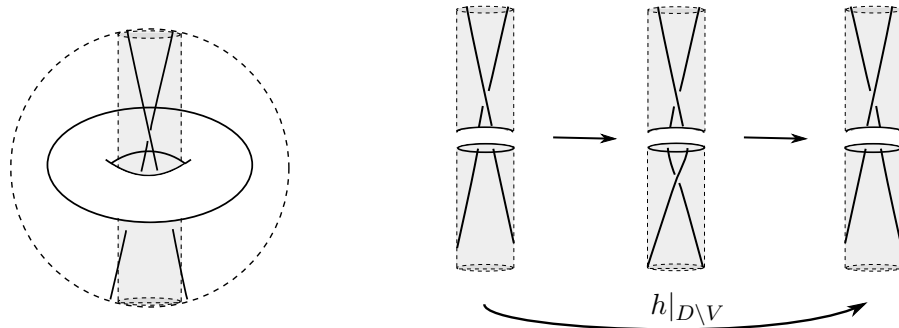


Figure 4.10: A homeomorphism of $D \setminus V$.

as required and is the identity along ∂D . Thus we can extend it by the identity on $\mathbb{R}^3 \setminus D$, obtaining the homeomorphism h . \square

Using this idea, we can change the crossings of any knot embedded in a solid torus T , by taking D to be a section of T containing the crossing in question, and $V \subset (\mathbb{R}^3 \setminus T)$ as shown:

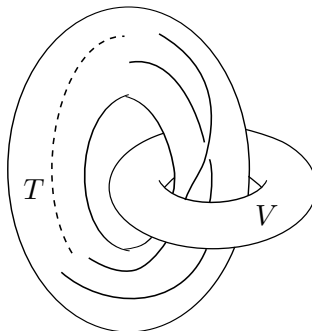


Figure 4.11: Given a knot embedded with a crossing in a solid torus T , choose V as shown and apply Proposition 4.2 to obtain a homeomorphism of $\mathbb{R}^3 \setminus V$ that switches the crossing.

This result will be used later, in the proof of Theorem 5.1.

4.2.2 Extending homeomorphisms of the boundary of a 3-manifold to its interior (minus some solid tori).

As the example of the solid torus suggests, we can learn about the homeomorphisms of 3-manifolds by examining homeomorphisms of their boundaries. In the general case, a homeomorphism of the boundary of a 3-manifold (which is a homeomorphism of a 2-manifold) can be extended to the interior of the 3-manifold, minus some solid tori [17, 20]. The following propo-

sition is necessary for the proof of Theorem 5.1. It also introduces the technique we will define in Section 5.1 as surgery.

Proposition 4.3. *Let h be a homeomorphism of the boundary of an orientable 3-manifold M . Then h can be extended to a homeomorphism $f : M \setminus (V_1 \cup \dots \cup V_n) \rightarrow M \setminus (V_1 \cup \dots \cup V_n)$, where $V_i \subset M$ are solid tori and $f|_{\partial M} = h$.*

Proof. Since M is an orientable 3-manifold, ∂M is compact, orientable and without boundary. So we know by the Dehn-Lickorish Theorem that $h : \partial M \rightarrow \partial M$ is isotopic to a composition of Dehn twists.

First, assume that h is isotopic to a single Dehn twist along some curve γ in ∂M . We cut out a solid torus V from M , and then extend h to $f : M \setminus V \rightarrow M \setminus V$. To construct V , let K be an ϵ -neighborhood on one side of γ in ∂M , such that h outside of K is the identity. Then push K slightly from ∂M into the interior of M . Let T be the interior half of the area it sweeps out, as shown in Figure 4.2.2.

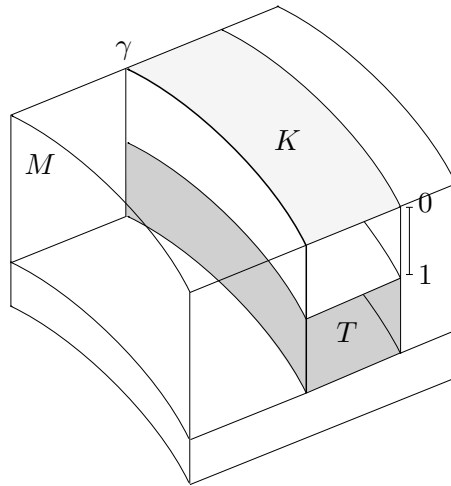


Figure 4.12: Drilling a hole T in M in preparation for defining a homeomorphism on $M \setminus T$.

Next, construct f to be a continuous extension of h in the area $D = K \times [0, 1]$ of the picture, and the identity elsewhere. In particular, on $\gamma \times [0, 1]$ and $(\gamma + \epsilon) \times [0, 1]$, f is the identity. Also, note that f is not the identity on $K \times \{1\}$, and so the removal of V is really necessary: f is a homeomorphism of $M \setminus V$, but not of M (since it would not be continuous on $K \times \{1\}$).

Finally, suppose h is isotopic to a composition of Dehn twists $h_1 \circ h_2 \circ \dots \circ h_n$. For each h_i , perform the construction above, taking care that V_i is chosen at such a depth that it does not

intersect any of the previously removed V_j . Each h_i is then extended to $f_i : M \setminus V_i \rightarrow M \setminus V_i$. So on $M \setminus (V_1 \cup \cdots \cup V_n)$, we can define $f_1 \circ \cdots \circ f_n$, which is isotopic to h on ∂M . \square

Chapter 5

Link Surgery

The Dehn-Lickorish theorem and the work of the previous chapter have Theorem 5.1 as an important corollary which allows us to define a process called surgery. Surgery techniques yield many examples of 3-manifolds that are homeomorphic to one another. Section 5.3 will use these tools, along with the material from Section 2.2 on covering spaces, to demonstrate two new methods of obtaining lens spaces.

5.1 The Dehn-Lickorish Corollary

Theorem 5.1. *Any compact orientable 3-manifold M^3 without boundary can be obtained by cutting unknotted solid tori from S^3 and regluing them along homeomorphisms of their boundaries.*

Proof. By Theorem 3.1, M^3 has a Heegaard splitting (M_1, M_2, f_1) , where M_1 and M_2 are g -handlebodies. Let (M_1, M_2, f_0) be a Heegaard splitting of S^3 into two g -handlebodies (guaranteed by Example 16). Then we have two homeomorphisms, f_0 and f_1 , from ∂M_1 to ∂M_2 . Define $f = f_1^{-1} \circ f_0 : \partial M_1 \rightarrow \partial M_1$, an automorphism of ∂M_1 . By Proposition 4.3, f can be extended to an automorphism h of $M_1 \setminus \bigcup V_i$, for $V_i \subset M_1$ solid tori.

Claim: $M^3 \setminus \bigcup V_i$ and $S^3 \setminus \bigcup V_i$ are homeomorphic. To prove this, construct a gluing j of $\partial(M_1 \setminus \bigcup V_i)$ and ∂M_2 that produces a manifold homeomorphic to $S^3 \setminus \bigcup V_i$, and show that this gluing is isotopic to f_1 . Define the following spaces:

$A = M_1 \setminus \bigcup V_i$, where M_1 comes from the Heegaard splitting of S^3 .

$A^* = M_1 \setminus \bigcup V_i$, where M_1 comes from the Heegaard splitting of M^3 .

$B = M_2$, where M_2 comes from the Heegaard splitting of S^3 .

$B^* = M_2$, where M_2 comes from the Heegaard splitting of M^3 .

Then there are maps $h : \partial A \rightarrow \partial A^*$, $f_0 : \partial A \rightarrow \partial B$, and $\text{id} : \partial B \rightarrow \partial B^*$. Define a gluing $j : \partial A^* \rightarrow \partial B^*$.

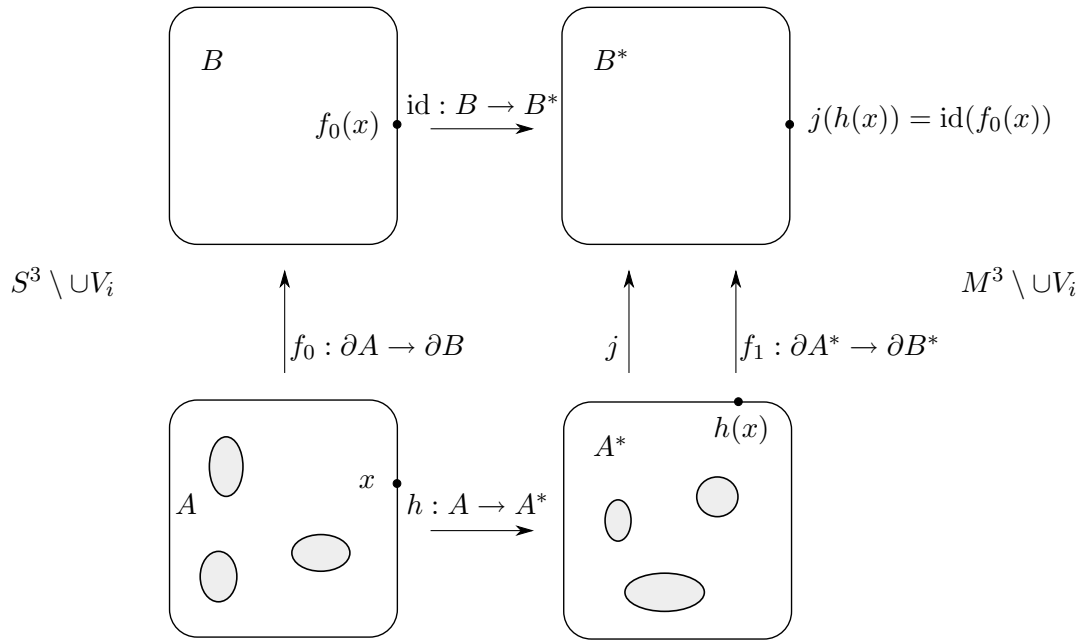


Figure 5.1: The spaces of Theorem 5.1, and the maps between them.

Let $x \in \partial A$. Define j such that $h(x)$ maps to $\text{id} \circ f_0(x)$; that is, $j = \text{id} \circ f_0 \circ h^{-1}$. Since id and h are homeomorphisms, the manifold $(S^3 \setminus \bigcup V_i)$ obtained by gluing ∂A and ∂B along f_0 is homeomorphic to the one obtained by gluing ∂A^* and ∂B^* along j . By definition, h is isotopic to $f = f_1^{-1} \circ f_0$ on ∂M_1 . So j is isotopic to $f_0 \circ (f_1^{-1} \circ f_0)^{-1} = f_1$, and the manifold obtained by gluing ∂A^* and ∂B^* along j is isotopic to $M^3 \setminus \bigcup V_i$.

Thus $M^3 \setminus \bigcup V_i$ and $S^3 \setminus \bigcup V_i$ are homeomorphic, so M_3 can be obtained from $S^3 \setminus \bigcup V_i$ by regluing the V_i along homeomorphisms of their boundaries.

Finally, the V_i must be unknotted. For, if one of the tori were knotted, any of its crossings could be reversed by homeomorphisms of S^3 (see Proposition 4.2), thereby unknotting it. \square

The definition of surgery formalizes the process above.

Definition 33. (K, r) surgery, or surgery with framing $r = \frac{p}{q}$ along a knot K , is the process of removing an open neighborhood of a knot K (a solid torus) from S^3 and regluing it by a homeomorphism of the boundary that takes the meridian to $\langle p, q \rangle$. We observe the convention that $r = 0$ implies $p = 0$ and $q = 1$, and $r = \infty$ implies $p = 1$ and $q = 0$.

Remark 11. The definition of preferred longitude from Section 4.2.1 is required here, as the choice of longitude would otherwise be unclear for nontrivial knots.

Remark 12. For a given K and r , (K, r) surgery determines a unique manifold. We know by Theorem 2.1 that p and q must be coprime, so there is a unique choice for p and q . When a solid torus V is glued into $S^3 \setminus V$ by some homeomorphism h , the resulting manifold is determined by the image of the meridian of V under this homeomorphism. Because one choice of longitude can be transformed into another by isotopy of the solid torus, the choice of the image of the longitude does not affect the manifold. And any two homeomorphisms h and h' mapping $\langle 1, 0 \rangle$ to $\langle p, q \rangle$ yield the same manifold: since any two curves of type $\langle p, q \rangle$ in the torus are isotopic (by Theorem 2.1), there must be an isotopy of an open neighborhood of ∂V taking the manifold obtained by h to the one obtained by h' .

Remark 13. Theorem 5.1 says that any compact orientable 3-manifold without boundary can be obtained by a series of (\bigcirc, r) surgeries.

Example 19. $(\bigcirc, 0) = S^1 \times S^2$. To see this, first remove an unknotted torus V_1 from S^3 . We already know (from Example 15) that $S^3 \setminus V_1$ is a second solid torus, and that they were attached by a homeomorphism $h : \partial V_1 \rightarrow \partial V_2$ that exchanges meridian and longitude. To reattach them, note that the framing of 0 means $p = 0$ and $q = 1$. So the homeomorphism $f : \partial V_1 \rightarrow \partial V_2$ given by the surgery also exchanges meridian and longitude. Thus f takes meridians (resp. longitudes) of V_1 to meridians (resp. longitudes) of V_2 , and it is isotopic to the identity homeomorphism on ∂V_1 .

So $(\bigcirc, 0)$ surgery glues two solid tori by the identity homeomorphism f of their boundaries. Each of the solid tori V_1 and V_2 can be written as $S^1 \times D^2$, and f glues together the boundaries of each D^2 (meridional disk of V_i). The gluing $\text{id} : \partial D^2 \rightarrow \partial D^2$ yields S^2 , so $f : \partial V_1 \rightarrow \partial V_2$ gives $S_1 \times S_2$.

The definition of surgery can be extended from knots to links by assigning a framing to each component of the link. If a link $L = \bigcup_{i=1}^n K_i$, we can write the surgery along L as $(L = \bigcup_{i=1}^n K_i; r_1, \dots, r_n)$. However, unless L is specified, this leaves ambiguity about how the components of the link are related to one another. For this reason, surgery along links is usually

represented by a diagram, as in the following example.

Example 20. $H = \text{Hopf link}$, with framings 1 and n . The diagram looks like this:

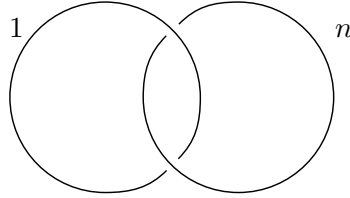


Figure 5.2: $(H = \bigcirc_1 \cup \bigcirc_2; 1, n)$ -surgery.

Proposition 5.1. *Any compact orientable 3-manifold without boundary can be obtained by surgery along a link with trivial components and integer framings.*

Proof. This follows directly from Theorem 5.1. The procedure used in the proof of Theorem 5.1 removes unknotted solid tori and reglues each of them along a homeomorphism of the boundary isotopic to Dehn twists. The fact that the tori are unknotted corresponds to $K = \bigcirc$ in a surgery presentation $(\bigcup K_i; r_1, \dots, r_n)$, and a Dehn twist takes $\langle 0, 1 \rangle$ to $\langle \pm 1, 1 \rangle$, which corresponds to a framing of ± 1 . \square

5.2 Link and Ribbon Presentations

As Example 20 suggests, surgery presentation isn't unique: different surgeries can give the same manifold (such surgeries are called *equivalent*). Through several examples, we classify some surgery presentations according to which manifolds they represent. To do this, we define a new way of depicting link surgery called a ribbon presentation.

Proposition 5.2. *Surgery by $(\bigcirc, \frac{p}{q})$ gives the Lens space $L(p, q)$.*

Proof. Recall from Example 17 that $L(p, q)$ is obtained by the Heegaard splitting of S^3 into two solid tori attached by a homeomorphism h of their boundaries, with the image of the meridian under h represented by $\langle q, p \rangle$. In terms of surgery, this means cutting a solid torus V from S^3 (attached by a homeomorphism g , where $g_*\langle 1, 0 \rangle = \langle 0, 1 \rangle$), performing a homeomorphism $f : \partial V \rightarrow \partial V$ with $f_*\langle 1, 0 \rangle = \langle p, q \rangle$, and then regluing V to S^3 by g . The framing of this surgery comes from the image of the meridian under f . Thus the surgery can be written $(\bigcirc, \frac{p}{q})$. \square

Proposition 5.2 and our knowledge of lens spaces yield results about surgery, like the following example, as easy corollaries.

Example 21. Surgery by (\mathbb{O}, r) is equivalent to surgery by $(\mathbb{O}, \frac{1}{n+\frac{1}{r}})$, for $n \in \mathbb{Z}$.

Proof. Let $r = \frac{p}{q}$. By Proposition 5.2, the above statement is equivalent to $L(p, q) = L(1, n + \frac{1}{r})$.

Recalling from Example 17 the definition of $L(p, q)$ as a quotient space of S^3 by $\sigma_{p,q}(z, w) = (ze^{2\pi i/p}, we^{2\pi i q/p})$, observe that $\sigma_{p,q} = \sigma_{p,q+pn}$. Thus,

$$L(p, q) = L(p, q + pn) = L(1, \frac{q}{p} + n) = L(1, n + \frac{1}{r}),$$

which proves our claim. □

The result of Example 21 implies the existence of a homeomorphism between manifolds M^3 , obtained by (\mathbb{O}, r) surgery, and N^3 , obtained by $(\mathbb{O}, \frac{1}{n+\frac{1}{r}})$ surgery. We now describe this homeomorphism, and see that it is a useful tool for manipulating surgery presentations.

Let $f : M^3 \rightarrow N^3$ be the homeomorphism required by Example 21. Write M^3 as the Heegaard splitting (V_1, V_2, h) of $L(p, q)$, where V_1 and V_2 are solid tori and $h_*\langle 1, 0 \rangle = \langle q, p \rangle$. Let D be a meridional disk of V_2 in general position, so that $h(m)$ (where m is the meridian) intersects D in p points.

Define f as the composition of n meridional Dehn twists (as defined in Section 4.2.1) of the solid torus V_2 along D (see Figure 5.2). Because f is a homeomorphism of V_2 , it does not change the manifold M^3 . Consider its effect on $h(m)$: as a meridional twist, f does not change the number of times $h(m)$ wraps around longitudinally. However, at each point where D intersects $h(m)$, f contributes n additional twists. We know there are p such points. Thus $(f \circ h)_*(m) = f_*\langle q, p \rangle = \langle q + pn, p \rangle$. (If n is positive (resp. negative), f will twist V_2 in the positive (resp. negative) direction, increasing (resp. decreasing) the number of times $f(h(m))$ wraps around V_2 meridionally.) So $f \circ h$ is the homeomorphism in a Heegaard splitting of N^3 into solid tori, and f is the required homeomorphism taking M^3 to N^3 .

Next, we show how to use the homeomorphism f to manipulate integer surgery presentations. Consider a surgery $(L_1, \dots, L_k; r_1, \dots, r_k)$, where $r_i \in \mathbb{Z}$. In a Heegaard splitting (V_1, V_2, h) of a 3-manifold M^3 , let V_1 be a neighborhood of L_1 (a solid torus). As shown above, the homeomorphism $f : M^3 \rightarrow M^3$ is a meridional twist on V_2 and the identity on V_1 . Applying f to the surgery presentation $(L_1, \dots, L_k; r_1, \dots, r_k)$ yields a new, equivalent surgery presentation.

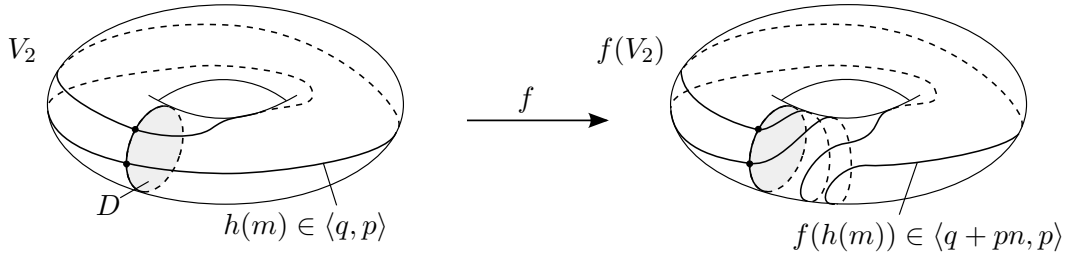


Figure 5.3: The effect of the homeomorphism $f : L(p, q) \rightarrow L(p, q + pn)$ on V_2 . In the example, $p = 2$, $q = 1$ and $n = -1$.

To determine this new surgery presentation, we must find the framings of L_i after performing f on M^3 (we call these new framings $f(r_1), \dots, f(r_k)$). The discussion above tells us that $f(r_1)$ is $\frac{r_1}{nr_1+1}$, since a twist of the meridian of V_2 is a twist of the longitude of V_1 .

To see how f changes the remaining r_i , we introduce ribbon presentations, an alternative way to show surgeries with integer framing.

Definition 34. Consider a surgery (K, r) with $r \in \mathbb{Z}$: that is, remove a neighborhood of the knot K (a solid torus V), and glue it back in along a homeomorphism h taking the meridian of V to a torus knot J of type $\langle r, 1 \rangle$. Let R be the narrow strip with boundary $J \cup K$. Then R is the *ribbon presentation* of (K, r) . Integer surgery along links can be transformed into a ribbon presentation in the same way, with one ribbon for each component of the link.

Remark 14. The framing r can be recovered from a ribbon presentation of (K, r) : it is $\text{lk}(J, K)$. Thus a ribbon presentation preserves all the information of a link presentation.

Next, use these ribbon presentations R_i of (L_i, r_i) to investigate the remaining r_i in the integer surgery presentation $(L_1, \dots, L_n; r_1, \dots, r_n)$. There are three possible ways R_i can be positioned in relation to L_1 :

1. If R_i does not pass through the center of V_1 , then it remains unchanged by f (so r_i also stays the same).
2. If R_i passes once through the center of V_1 , then f performs n full twists on R_i . Each twist changes the linking number of L_i and J_i by one, so r_i becomes $r_i + n$.
3. Suppose R_i passes through the center of V_1 more than once. In particular, we can assign an orientation to R_i , and then count the number of times it passes through the center of V_1 in each direction. Let R_i pass through the center of V_1 s times in one direction, and t times in the other. The effect of a single meridional twist of V_2 on R_i is pictured

below:

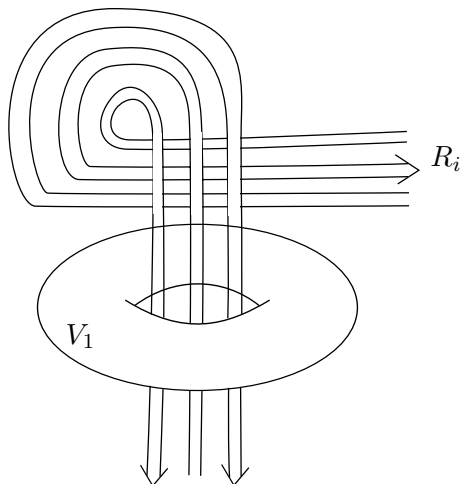


Figure 5.4: The effect of a meridional twist of V_2 on the ribbon R_i passing through the center of V_1 .

To find r_i , we must calculate $\text{lk}(J, K)$. Selecting one edge of R_i to follow, notice that each time it passes over a strand oriented in the same (resp. opposite) direction, $\text{lk}(J, K)$ increases (decreases) by one. Counting up all the crossings, then:

- Each of the t upward-oriented strands passes over all t of the upward-oriented strands, adding t^2 to $\text{lk}(J, K)$. And each of the s downward-oriented strands passes over all s of the downward-oriented strands, adding s^2 to $\text{lk}(J, K)$.
- Each of the t upward-oriented strands passes over all s of the downward-oriented strands, subtracting ts from $\text{lk}(J, K)$. And each of the s downward-oriented strands passes over all t of the upward-oriented strands, subtracting st from $\text{lk}(J, K)$.

Thus, r_i becomes $r_i + (t^2 + s^2 - ts - st) = r_i + (s - t)^2$. Note that $s - t = \text{lk}(L_1, K)$. So f transforms r_i into $r_i + \text{lk}(L_1, K)^2$.

Example 22. The surgery presentations in diagrams (A) and (D) of Figure 22 are equivalent.

In diagram (B), we add a surgery along a trivial knot with framing ∞ . This yields a manifold homeomorphic to the one given by the surgery presentation in diagram (A), since surgery with framing ∞ takes meridians to meridians and longitudes to longitudes (that is, it's isotopic to the identity).

In diagram (C), we have performed a single twist along the newly created trivial knot J to

create a new surgery presentation of the same manifold given by diagrams (A) and (B). This changes the framing of the trivial knot, as demonstrated above, to $\frac{1}{\infty+1} = 1$. We add $\text{lk}^2(J, K)$ to the framing of the second component K . But the $\text{lk}(J, K) = 0$, so the framing of K does not change. Straightening the strands of K , we obtain figure (D).

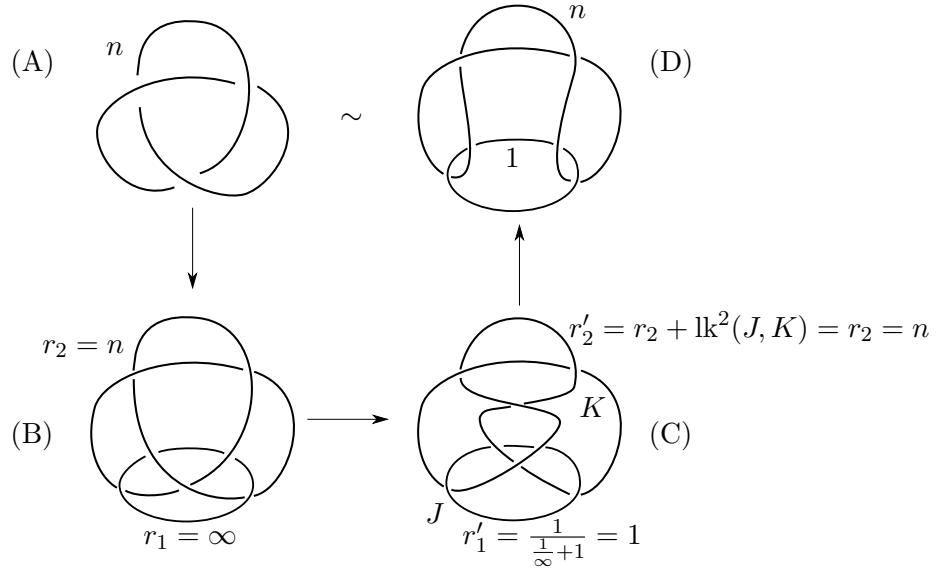


Figure 5.5: A manipulation of link presentations showing that the surgeries given by diagrams (A) and (D) are equivalent.

Examples 22 and 23 are only two of the many results about equivalence of surgery presentations that use the tools of the discussion above. (For others, see [17, 20].)

5.3 Lens spaces, surgery, rational links and covering spaces: two examples

In this section, we demonstrate two more ways to obtain lens spaces. The first uses the surgery techniques of the previous section. The second generalizes the classification of rational tangles mentioned in Chapter 2.

Proposition 5.3. *The following surgery yields $L(p, q)$:*

.

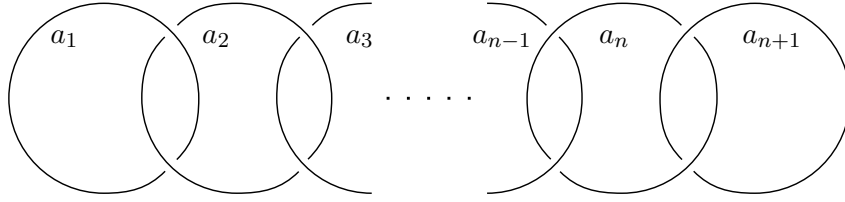


Figure 5.6: This surgery gives $L(p, q)$, where $\frac{p}{q}$ is defined below.

$$\text{where } \frac{p}{q} = a_1 - \frac{1}{a_2 - \frac{1}{a_3 - \dots - \frac{1}{a_n - \frac{1}{a_{n+1}}}}}$$

Proof. We begin by describing a two-step procedure:

1. Twist by $-a_n - 1$ along the $(n + 1)$ -th component. The framing a_n becomes -1 , a_{n-1} becomes $\frac{1}{-a_n - 1 + \frac{1}{a_{n+1}}}$, while the other a_i remain constant.
2. Next, twist once along the n th component. The framing of this circle then becomes ∞ (and surgery along a trivial knot with framing ∞ is the identity), so it is discarded. The framing of the rightmost component (now the n th circle) and the adjacent component (the $(n - 1)$ th circle) each increase by one. Thus a_{n-1} becomes $a_{n-1} + 1$, and a_n becomes

$$1 + \frac{1}{-a_n - 1 + \frac{1}{a_{n+1}}} = \frac{1}{1 + \frac{1}{a_n - \frac{1}{a_{n+1}}}}$$

Repeating these two steps, obtain a new $a_{n-2} = a_{n-2} + 1$, and a_{n-1} becomes

$$\frac{1}{1 + \frac{1}{a_{n-1} - \frac{1}{a_n - \frac{1}{a_{n+1}}}}}$$

After $n + 1$ such repetitions, then, the result is a single trivial loop with framing

$$\frac{1}{1 + \frac{1}{a_1 - \frac{1}{a_2 - \frac{1}{a_3 - \dots}}}} = \frac{1}{1 + \frac{1}{\frac{p}{q}}}, \text{ where } \frac{p}{q} = a_1 - \frac{1}{a_2 - \frac{1}{a_3 - \dots - \frac{1}{a_n - \frac{1}{a_{n+1}}}}}, \text{ as required.}$$

□

The following discussion gives our final example of a method for constructing lens spaces: as branched coverings of S^3 over rational links.

Definition 35. Recall from Section 2.2 that a *rational link* is a link that can be composed into two rational tangles (equivalently, a rational link can be constructed by joining the ends of a rational tangle).

A projection of a nontrivial link onto the plane necessarily has crossings. By lifting arcs of a link out of the plane, these crossings can be removed. When the projection of the arcs onto the plane is a set of n disjoint straight line segments, this process is called adding bridges to obtain an *n-bridge presentation*. A proof of the following proposition can be found in [3]:

Proposition 5.4. *Every rational link has a 2-bridge presentation.*

□

We next define the 2-fold branched cyclic cover of a solid ball over two unknotted arcs.

Let M be an orientable surface embedded in S^3 with boundary K (this is called a *Seifert surface* for K : see [3, 20] for further discussion.) Let $N = N^+ \cup N^-$ be an open neighborhood of M in S^3 , where $\partial N^+ \cap \partial N^- = M$, as shown in Figure 5.3. Let $Y = S^3 \setminus M$, and $X = S^3 \setminus K$. Make two copies N_1 and N_2 of N and two copies Y_1 and Y_2 of Y .

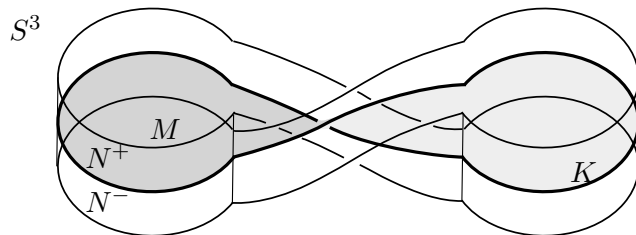


Figure 5.7: The knot K , its Seifert surface M , and the neighborhood $N = N^+ \cup N^-$ in S^3 .

Definition 36. The 2-fold unbranched cyclic cover of $S^3 \setminus K$ is the space \tilde{X} formed by identifying $N_i^+ \subset Y_i$ with $N_i^+ \subset N_i$, and $N_i^- \subset Y_i$ with $N_{i+1}^- \subset N_{i+1}$ (modulo 2). The natural map $p : \tilde{X} \rightarrow X$ is a covering map.

From this unbranched cyclic cover, we next create a branched cyclic cover. Let N be an open neighborhood of K in S^3 , and construct the 2-fold unbranched cyclic covering $p : \tilde{X} \rightarrow S^3 \setminus N$. Both ∂N and $\partial(p^{-1}(N))$ are tori. Note that the preimage of a meridian of ∂N is a single meridian in $\partial(p^{-1}(N))$, while the preimage of a longitude of ∂N consists of two disjoint longitudes of $\partial(p^{-1}(N))$.

Glue a solid torus V to $\partial(p^{-1}(N))$ by a homeomorphism taking meridians to meridians. We now extend p to a branched covering of S^3 by $M^3 = V \cup \partial(p^{-1}(N))$ over K in the following way. For $z = (e^{i\theta}, e^{i\phi}, r) \in V = D^2 \times S^1$, let $z \mapsto (e^{2i\theta}, e^{2i\phi}, \frac{r}{|z|})$.

Definition 37. Given a continuous map $p : Y \rightarrow X$, let B be the points in X on which p is an even cover. If B is a proper submanifold of X , and $p^{-1}(B) = A$ is a proper submanifold of Y , then p is a *branched covering*. B and A are called the *branch sets* of the covering map p .

So the map $f(z) = \begin{cases} p(z) & \text{if } z \in M^3 \setminus V \\ (e^{2i\theta}, e^{2i\phi}, \frac{r}{|z|}) & \text{if } z \in V \end{cases}$ is a branched covering, with branch sets $K \subset S^3$ and $A \subset M^3$.

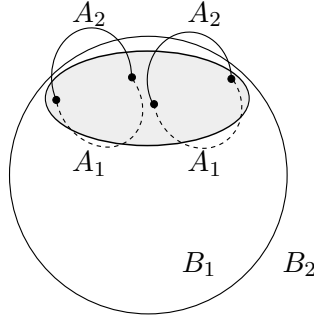


Figure 5.8: A Heegaard splitting of S^3 into balls B_1 and B_2 , which intersect the knot K in pairs of segments A_1 and A_2 .

Let K be a rational link embedded in S^3 . Then K is 2-bridged, so it can be divided into 4 unknotted, unlinked segments: the two bridges and the segments in between. Consider (B_1, B_2, h) , a Heegaard splitting of S^3 such that $A_1 = B_1 \cap K$ and $A_2 = B_2 \cap K$ each consist of two of the unknotted, unlinked segments of K (see Figure 5.3).

Then the 2-fold branched cyclic cover f of S^3 over K is a Heegaard splitting $M^3 = (f^{-1}(B_1), f^{-1}(B_2), \tilde{h})$,

and $f^{-1}(B_1)$ and $f^{-1}(B_2)$ are solid tori (branched cyclic covers of B_i). To understand M^3 , it remains to determine how \tilde{h} glues $f^{-1}(B_1)$ and $f^{-1}(B_2)$ together. We consider three cases:

1. If h_0 is the identity on ∂B_1 , then \tilde{h}_0 is the identity on $\partial(f^{-1}(B_1))$. So K is the trivial 2-component link, and $M^3 = L(0, 1) = S^2 \times S^1$ (as we know from Example ??).
2. Let h_1 be the homeomorphism of ∂B_1 that changes A_1 as shown. Then Figure 2 demonstrates that \tilde{h}_1 is a longitudinal twist. So M^3 (obtained by gluing two solid tori along \tilde{h}_1) is $L(1, 1)$.

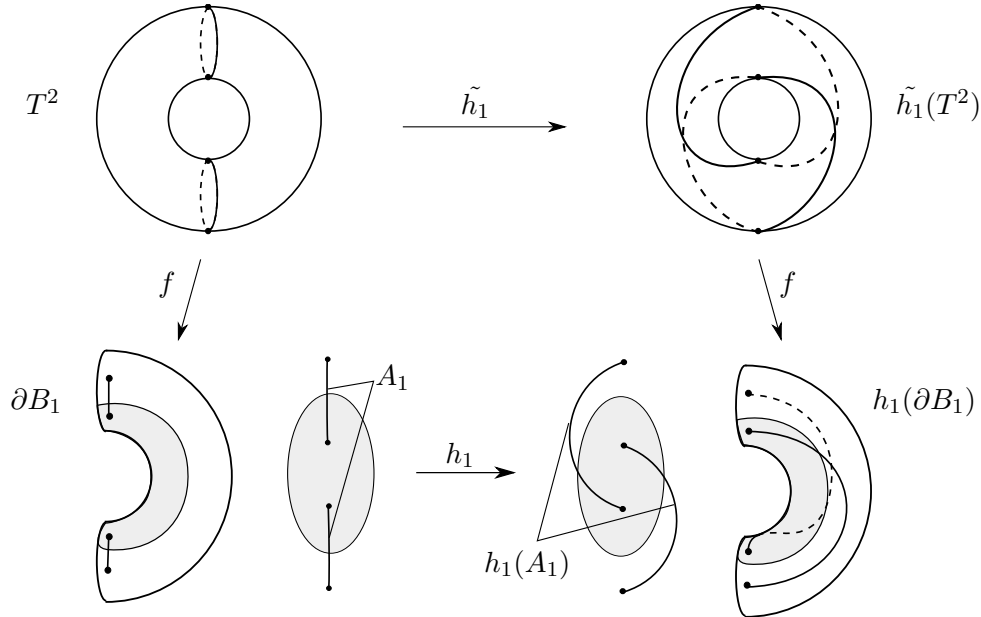


Figure 5.9: An automorphism h_1 of S^2 and its preimage $\tilde{h}_1 \in \text{Aut}(T^2)$ under the covering map $f : T^2 \rightarrow S^2$.

3. By a similar process, the homeomorphism h_2 shown in Figure 3 gives a meridional twist \tilde{h}_2 . So $M^3 = L(0, 1)$.

Using h_1 and h_2 , we can create any 2-bridge knot K , and we know how the boundaries of the corresponding $f^{-1}(B_i)$ are glued together, and thus which lens space is obtained.

To illustrate this, we construct the 2-fold branched cyclic covering of S^3 over the knot K shown in Figure 5.3 (this rational link is the closure of the rational tangle in Figure 2.13.). Note that K contains three sets of twists: +3 twists of the middle two points, -2 twists of the leftmost two, and then +5 twists of the middle two. We say K has *twist coefficients* 3, -2, 5.

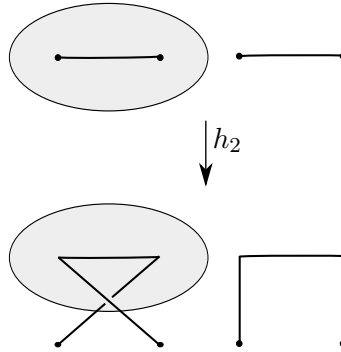


Figure 5.10: A homeomorphism h_2 of ∂B_1 , which yields a meridional twist of ∂T^2 .

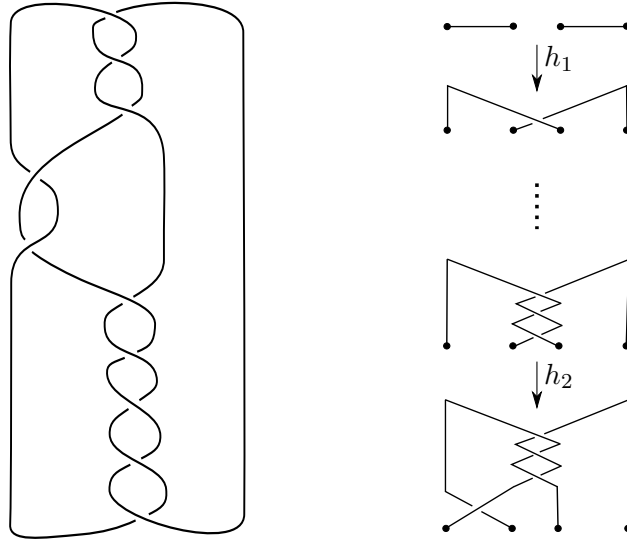


Figure 5.11: We construct a covering of S^3 over the knot K at left. At right, several steps in the sequence of homeomorphisms of B_1 needed to change A_1 into K .

We obtain K from the trivial 2-link by repeated application of steps 2 and 3 above. In particular, we have the homeomorphism $h = h_1^5 \circ h_2^{-2} \circ h_1^3 : \partial B_1 \rightarrow \partial B_1$. Since $\tilde{h} : \partial(f^{-1}(B_1)) \rightarrow \partial(f^{-1}(B_1))$ is an element of $\text{Aut}(\partial(f^{-1}(B_1))) = \text{Aut}(\partial T^2)$, we know from Section 2.2 that \tilde{h} represents an element of $\text{GL}(2, \mathbb{Z})$. Specifically,

$$[\tilde{h}] = \begin{pmatrix} 1 & 0 \\ 5 & 1 \end{pmatrix} \begin{pmatrix} 1 & -2 \\ 0 & 1 \end{pmatrix} \begin{pmatrix} 1 & 0 \\ 3 & 1 \end{pmatrix} = \begin{pmatrix} -5 & -2 \\ -22 & -9 \end{pmatrix}.$$

Thus M^3 is the union of two solid tori, glued along their boundaries by a homeomorphism taking the meridian to a curve of type $\langle -5, -22 \rangle$. That is, $M^3 = L(-5, -22) = L(5, 2)$.

Remark 15. Note that the framing $r = \frac{22}{5}$ of the surgery described above can also be written $\frac{22}{5} = 5 + \frac{1}{-2+\frac{1}{3}}$, where 5, -2 and 3 were the twist coefficients of K . This suggests the following general fact, stated here without proof (see [2, 17, 20] for further discussion):

Proposition 5.5. *The 2-fold branched covering of S^3 over the knot with twist coefficients*

$$a_1, a_2, \dots, a_k \text{ is } L(p, q), \text{ where } \frac{p}{q} = a_1 + \frac{1}{a_2 + \frac{1}{\dots + \frac{1}{a_k}}}. \quad \square$$

In Chapter 2, we constructed a map from the rational tangles to the automorphisms of T^2 , thereby reaching a classification of rational tangles. In this section, we have constructed a map from the rational links to lens spaces, which allows us to classify two rational links as equivalent if their associated lens spaces are homeomorphic.

Chapter 6

Conclusion

Some of the results we have shown here classify sets of 3-manifolds obtained by particular constructions. For example, we showed that the manifold obtained by $(\bigcirc, \frac{p}{q})$ surgery is homeomorphic to $L(p, q)$. Given what we know about lens spaces, we then have information about when two 3-manifolds obtained by (\bigcirc, r_1) and (\bigcirc, r_2) surgeries are homeomorphic. However, these results are very specific. More generally, it is possible to classify all 3-manifolds according to the type of geometry they admit. This theory can be found in [22, 24]. In this thesis, we have considered only one of the types of 3-manifold discussed there: Seifert-fibered 3-manifolds.

Lens spaces have appeared throughout this thesis as illustrations of many of its main ideas. Below is a summary of the contexts in which we have seen them.

- In Section 1.2.3, we defined lens spaces as the result of a covering map from S^3 under a group action σ .
- In Section 3.3, we proved that the definition of a lens space as a quotient space of S^3 under a group action is equivalent to the definition as a Heegaard splitting of two solid tori. Using the quotient space definition, we identified conditions under which two lens spaces are homeomorphic.
- In Section 5.2, we showed that the surgery presentation $(\bigcirc, \frac{p}{q})$ gives the lens space $L(p, q)$. We then used this result as a tool to better understand link presentations of surgery.
- Many surgery presentations are equivalent, and in Section 5.3 we saw another presentation, along a link with many components, that yields $L(p, q)$.

- Finally, in Section 5.3, we expressed lens spaces as branched covers of S^3 over a rational link — a fact which leads to a classification of rational links.

The surgery techniques developed in Chapters 4 and 5 are formalized in the Kirby calculus, which lies at the intersection of 3-manifold theory and 4-manifold theory [5, 13, 18], and they have a wide variety of applications. For example, surgery presentations can be used to define the Poincaré sphere: a famous example of a 3-manifold with the same homology groups as S^3 but a different fundamental group. The Poincaré sphere is a counterexample to the statement that all compact 3-manifolds with the same fundamental group as S^3 are homeomorphic to S^3 — an idea that Poincaré later modified into the still-unsolved Poincaré conjecture [10, 17, 20, 21].

Bibliography

- [1] M.A. Armstrong. *Basic Topology*. Springer, New York, 1983.
- [2] J. H. Conway. An enumeration of knots and links, and some of their algebraic properties. *Computational Problems in Abstract Algebra*, pages 329–358, 1967.
- [3] Peter Cromwell. *Knots and Links*. Cambridge University Press, Cambridge, United Kingdom, 2004.
- [4] P.H. Doyle and D.A. Moran. A short proof that compact 2-manifolds can be triangulated. *Invent. Math.*, 5:160–162, 1968.
- [5] R. Fenn and C. Rourke. On kirby’s calculus of links. *Topology*, 18(1):1–15, 1979.
- [6] William Fulton. *Algebraic Topology: A First Course*, volume 153 of *Graduate Texts in Mathematics*. Springer-Verlag, New York, 1995.
- [7] N.D. Gilbert and T.Porter. *Knots and Surfaces*. Oxford University Press, New York, 1994.
- [8] J. R. Goldman and L. H. Kauffman. Rational tangles. *Adv. in Appl. Math.*, 18:300–332, 1997.
- [9] Sue E. Goodman. *Beginning Topology*. Brooks/Cole, Belmont, CA, 2005.
- [10] John Hempel. *3-Manifolds*. Number 86. Princeton University Press, Princeton, NJ, 1976.
- [11] L.H. Kauffman. The conway polynomial. *Topology*, 20:101–108, 1981.
- [12] L.H. Kauffman and S. Lambropoulou. On the classification of rational tangles. *Adv. in Appl. Math.*, 33(2):199–237, 2004.

- [13] Robion C. Kirby and Laurence R. Taylor. A survey of 4-manifolds through the eyes of surgery. In *Surveys on surgery theory, Vol. 2*, volume 149 of *Ann. of Math. Stud.*, pages 387–421. Princeton Univ. Press, Princeton, NJ, 2001.
- [14] W. B. R. Lickorish. A representation of orientable combinatorial 3-manifolds. *Ann. of Math.*, 76:531–540, 1962.
- [15] Charles Livingston. *Knot Theory*. Number 24 in The Carus Mathematical Monographs. Mathematical Association of America, Washington, DC, 1993.
- [16] James R. Munkres. *Topology*. Prentice Hall, Inc., Upper Saddle River, NJ, 1975.
- [17] V. V. Prasolov and A. B. Sossinsky. *Knots, Links, Braids and 3-Manifolds: An Introduction to the New Invariants in Low-Dimensional Topology*, volume 154 of *Translations of Mathematical Monographs*. American Mathematical Society, Providence, Rhode Island, 1996.
- [18] A.I. Stipsicz R. E. Gompf. *4-Manifolds and Kirby Calculus*, volume 20 of *Grad. Studies in Math*. Amer. Math. Soc., 1999.
- [19] K. Reidemeister. *Knot Theory*. BCS Associates, Moscow, Idaho, 1983.
- [20] Dale Rolfsen. *Knots and Links*. Publish or Perish, Inc., Berkeley, California, 1976.
- [21] Nikolai Saveliev. *Lectures on the Topology of 3-Manifolds: An Introduction to the Casson Invariant*. Walter de Gruyter, Berlin, 1999.
- [22] Peter Scott. The geometries of 3-manifolds. *Bull. London Math. Soc.*, 15:401–487, 1983.
- [23] C. Sundberg and M. B. Thistlethwaite. The rate of growth of the number of prime alternating links and tangles. *Pacific J. Math.*, 182:329–358, 1998.
- [24] William P. Thurston. *Three-Dimensional Geometry and Topology*, volume 1. Princeton University Press, Princeton, New Jersey, 1997.
- [25] J.H.C. Whitehead. On C1-complexes. *Ann. of Math.*, 41(4):809–824, 1940.